T.C.

AKSARAY UNIVERSITY

GRADUATE SCHOOL OF NATURAL AND APPLIED SCIENCE

DEPARTMENT OF ELECTRICAL-ELECTRONIC AND COMPUTER ENGINEERING

DETECTION OF PHOTOVOLTAIC PANEL FAULTS WITH THERMAL CAMERA AND UV LED

Ph.D. THESIS

ATIL EMRE COŞGUN

SUPERVISOR

Prof. Dr. MEHMET REŞIT TOLUN

AKSARAY, 2020

Aksaray University, Graduate School of Natural and Applied Sciences Approval, Atıl Emre COŞGUN, Doctor of Philosophy with thesis, Student No. 162353303 successfully presented the Doctor of Philosophy Thesis titled "**DETECTION OF PHOTOVOLTAIC PANEL FAULTS WITH THERMAL CAMERA AND UV LED**", prepared after satisfying all the requirements identified in the concerned bylaws, before the jury whose signatures are affixed below.

Thesis Advisor: Prof. Dr. Mehmet Reşit TOLUN
Konya Food and Agricultural University
I approve that this thesis is a Doctor of Philosophy in scope and quality ....

Member: Assoc. Prof. Dr. İsmail BAYRAKLI
Aksaray University
I approve that this thesis is a Doctor of Philosophy in scope and quality ....

Member: Assoc. Prof. Dr. Emre ARSLAN
Aksaray University
I approve that this thesis is a Doctor of Philosophy in scope and quality ....

Member: Asst. Prof. Dr. Abdül Kadir GÖRÜR
Çankaya University
I approve that this thesis is a Doctor of Philosophy in scope and quality ....

Member: Asst. Prof. Dr. Abdülsamed TABAK
Necmettin Erbakan University
I approve that this thesis is a Doctor of Philosophy in scope and quality ....

Date of Defence: 25/06/2020

I agree that this thesis which is accepted by the jury, has fulfilled the requirements for being a Doctor of Philosophy Thesis.

....

Assoc. Prof. Dr. Mehmet Ali HINIS
Director of Natural and Applied Science

PLAGIARISM PAGE

I hereby declare that all information in this thesis has been obtained and presented in accordance with academic rules and ethical conduct. I also declare that, as required by these rules and conduct, I have fully cited and referenced all material and results that are not original to this work; otherwise I accept all legal responsibility.

ATIL EMRE COŞGUN

ACKNOWLEDGMENTS

First of all, I would like to express my deepest appreciation to my supervisor, Prof. Dr. Mehmet Reşit TOLUN, who gave me this great research opportunity. I am heartily thankful to him for his tireless guidance, extraordinary patience and constant encouragement during my academic journey. His knowledge, creativity and passion not only inspire me during my graduate studies, but also enlighten my future career. Without his persistent help, this dissertation would not have been possible.

I would like to thank my committee members, Assoc.Prof. İsmail BAYRAKLI and Assist. Prof. Dr. Abdul Kadir GÖRÜR who examined my dissertation and provide me so many valuable suggestions.

Finally, I am grateful to all my family members, especially my wife Ayşegül AKINCI COŞGUN and my daughter Nisa Nur COŞGUN, my father Hakkı COŞGUN, my mother Nihal COŞGUN, and my brother Bilal Ahmet COŞGUN and my sister Elif SEZER for always believing in me and encouraging me to do my best. All of their love, support, and sacrifices over these past years gave me the strength and determination to make my dreams come true.

ATIL EMRE COŞGUN
AKSARAY, 2020

TABLE OF CONTENTS

Ph.D. THESIS

DETECTION OF PHOTOVOLTAIC PANEL FAULTS WITH THERMAL CAMERA AND UV LED

Atıl Emre COŞGUN

Aksaray University
Graduate School of Natural and Applied Sciences
Department of Electrical Electronic and Computer Engineering

Supervisor: Prof. Dr. Mehmet Reşit TOLUN

ABSTRACT

In this thesis, hot spot failures, panel surface fractures, and yellowing problems on 40 Watt polycrystalline photovoltaic (PV) panel were analysed through indoor laboratory experiments and outdoor fieldwork. The outdoor field tests were performed with a 40 Watt PV panel on a clear and sunny day in the garden of Ortaköy Vocational School of Aksaray University. It is observed that the output power value of the panel decreases in the open circuit fault which was created by disconnecting the series-connected cells within the panel. In addition to the observed change in the power value, temperature increase value due to broken glass surfaces and disconnected cells on the panel was observed with a thermal camera. In the indoor laboratory experiments, artificial shading and yellowing parts detection studies were performed with UV LED and photodiode which is designed as a rectangular prism and placed at 45-degree angles. To perform these works on the photovoltaic (PV) panel, the user interface was developed and the graphical values of the manually scanned panel were plotted on the screen. Besides, colour changes on the PV panel were tried to be determined at different spectrum values. Blue, green, yellow and red LED have been used to do this. It is understood from the figure that the blue led spectrum is most effective method to obtain PV diagnosis. According to the results obtained, colour changes on the PV panel could not be obtained in colours other than blue. Additionally, common faults in PV systems which are shading situation, line to line faults, panel soiling problem, increasing resistance value problem between panels, problems caused by bird droppings or tree leaves and branches, and the effect of temperatures on the photovoltaic (PV) panels were simulated, analysed, and P-V and I-V graphics of the panels were drawn.

Keywords: Photovoltaic panel, PV panel faults, UV, thermal inspection.

June, 2020; 84 pages

DOKTORA TEZİ

FOTOVOLTAİK PANEL HATALARININ TERMAL KAMERA VE UV LED İLE TESPİTİ

Atıl Emre COŞGUN

Aksaray Üniversitesi
Fen Bilimleri Enstitüsü
Elektrik Elektronik ve Bilgisayar Mühendisliği Anabilim Dalı

Danışman: Prof. Dr. Mehmet Reşit TOLUN

ÖZET

Bu tez çalışmasında 40 Watt gücündeki polycristal fotovoltaik (FV) panellerde hot spot arızaları, panel yüzey kırıkları, sararma problemleri iç ortam laboratuvar deneyleri ve dış ortam saha deneyleri ile incelenmiştir. Dış ortam deneyleri, Aksaray Üniversitesi, Ortaköy Meslek Yüksek Okulu bahçesinde 40 Watt gücündeki fotovoltaik (FV) panel ile havanın açık ve güneşli olduğu bir günde gerçekleştirilmiştir. Panel içindeki seri bağlı hücrelerin bağlantısı kesilerek oluşturulan açık devre hatasında panelin çıkış güç değerinin düştüğü gözlemlenmiştir. Güç değerindeki değişimin yansıra panel üzerindeki kırılmış cam yüzeyleri ve bağlantısı kesilmiş hücrelerden kaynaklı sıcaklık artış değeri Termal kamera ile gözlemlenmiştir. İç ortam laboratuvar deneylerinde, bir kutu dikdörtgen prizması şeklinde tasarlanan ve 45 derecelik açılarla yerleştirilen UV LED ve foto diyot ile yapay gölgeleme ve sarı bölge tespit çalışmaları yapılmıştır. Fotovoltaik (FV) panel üzerinde bu çalışmaları gerçekleştirmek için kullanıcı ara yüzü geliştirilmiş ve el ile taranan panelin grafik değerleri ekrana çizdirilmiştir. Bununla birlikte farklı dalga boylarına sahip LED ışık kaynakları (mavi, yeşil, kırmızı ve sarı) ile panel üzerindeki renk değişimleri tespit edilmeye çalışılmıştır. Elde edilen sonuçlara göre en etkili yöntemin mavi led ile panel üzerindeki renk değişiminin tespiti olduğu gözlemlenmiştir. Ayrıca mavi led dışında kalan renklerin hata tespitinde etkili olmadığı grafiklerde gözlemlenmiştir. Bu çalışmaların yanında PV sistemlerde sıklıkla karşılaşılabilecek hatalar; gölgelenme durumu, bağlantı hataları, panel üstü kirlenme sorunu, yıllar geçtikçe paneller arasında artan direnç değer problemi, kuş pisliklerinden veya ağaç yaprak ve dallarından kaynaklanan problemler ile sıcaklıkların fotovoltaik (FV) paneller üzerindeki etkisi ön benzetim programları senaryolaştırılmış ve panellerin P-V ve I-V grafikleri çizdirilmiştir.

Anahtar Kelimeler: Fotovoltaik panel, fotovoltaik panel hataları, UV, termal denetim.

Haziran, 2020; 84 sayfa

LIST OF FIGURES

LIST OF TABLES

ABBREVIATIONS

A	diode quality factor
AC	alternating current
AI	artificial intelligence
CMM	comparison between measured and modeled
DC	direct current
FDC	fault detection and classificatio
G	Irradance (W/m2)
GEPA	Solar Energy Potential Atlas
I	current(A)
$\mathbf{I_{SC}}$	short circuit current(A)
$\mathbf{I_{D1}}$	diode current(A)
k	boltzmann's constant
P	power
PV	photovoltaic
RES	renewable energy source
$\mathbf{R_{S}}$	series resistance
T	temperature
STC	standard test conditions
UV	ultraviole
V	voltage(V)
$\mathbf{V_{bat}}$	battery voltage
Vg	grid voltage
$\mathbf{V_{MPP}}$	voltage at maximum power point
$\mathbf{V_{OC}}$	open-circuit voltage(V)

1. INTRODUCTION

Today, one of the most important sources of alternative energy sources is solar energy. According to the Turkey's Solar Energy Potential Atlas (GEPA), the annual sunshine time of 2.737 hours (total daily 7.5 hours) and the annual total solar energy 1.527 kWh/m² are due to the geographical location of Turkey. GEPA is illustrated in Figure 1. Also, Turkey's total solar energy potential for each month is illustrated in Table 1.

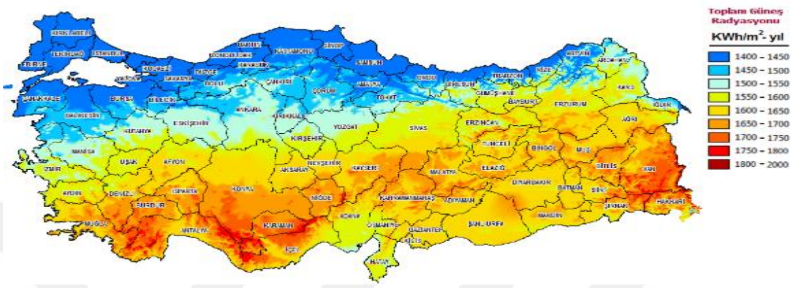

Figure 1.1. Turkey's Solar Energy Potential Atlas (GEPA)[1].

Table 1.1. Turkey's total solar energy potential for each month.

Months	Total solar energy per month		Sunshine Duration
	kcal/cm^2-month	kWh/m^2-month	
January	4.45	51.75	103
February	5.44	63.27	115
March	8.31	96.65	165
April	10.51	122.23	197
May	13.23	153.86	273
June	14.51	168.75	325
July	15.08	175.38	365
August	13.62	158.4	343
September	10.60	123.28	280
October	7.73	89.9	214
November	5.23	60.82	157
December	4.03	46.87	103
Total	**112.74**	**1311.16**	**2640**
Average	**308 Cal/cm^2**	**3.6kWh/m^2-day**	**7.2 hour/day**

According to the International Energy Agency's Renewables 2019 market report, total renewable-based power capacity in the world will grow by 50% between 2019 and 2024 to meet this energy need. It is predicted that half of this growth will constitute pv market [2], although improvement is provided about hybrid energy system [3]. Figure 1 shows the PV panel installation capacity during the last 10 years. In 2019, the net installed capacity was 580.159 MW. When compared to the previous year, the increase rate was about 20%.

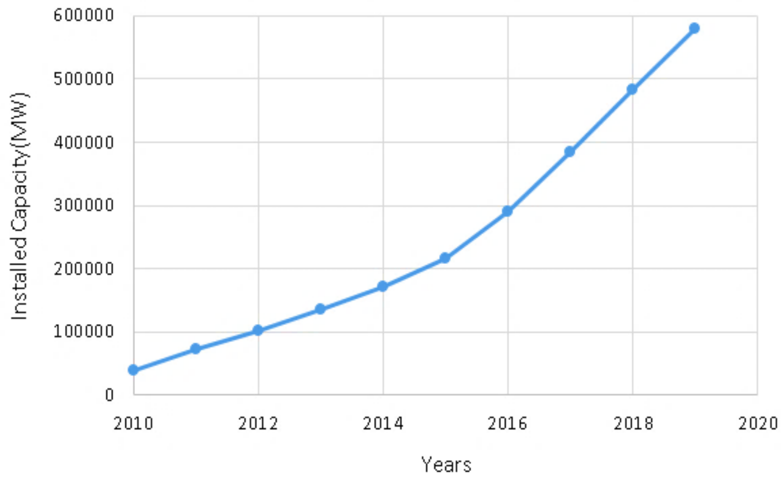

Figure 1.2. PV Panels Installations capacity between 2010 and 2019 [4].

PV modules are formed by connecting an array of solar cells in series and in parallel. Depending on the used materials in the PV cells, its efficiency and cost increase or decrease. There are some experimental PV cells that have an efficiency of nearly 40% [5]. However, the average energy conversion efficiency is about 10%-25% in the field used PV modules [6-8]. Today, monocrystalline silicon, polycrystalline silicon, amorphous silicon, Cadmium telluride and copper indium selenide/sulfide are generally used as materials for solar cells [9].Organic PV modules based on GaAs are also available in the market. High efficiency energy harvesting could be obtained from GaAs based organic module by using infrared transparency window between the 650 nm and 950 nm wavelength range [10]. Operational lifetime of photovoltaic (PV) modules is over 20 years [11-14]. However, photovoltaic (PV) modules are exposed to different external stresses that can affect functional properties and lead to reduced solar cell performance [14, 15]. According to photovoltaic module manufacturers at 1000 W/m2, a temperature of 25°C, and the air mass of 1.5 a PV module gives the maximum performance. These parameters are used by many researchers as a standard test condition (STC) in their studies. The current literature shows that studies on the photovoltaic (PV) module degradation is increasing [15-20]. Ethylene Vinyl Acetate (EVA) is the most commonly used backsheet encapsulation material in PV modules [21]. Although elevated temperature and UV irradiation decreases stabilizer concentration gradually, using UV stabilizers and antioxidants may affect its operational life positively [22]. External factors such as UV irradiation, thermal changes, and humidity are the reason of degradation and aging of PV modules. The widely observed defects in the field PV modules include EVA yellowing, EVA browning, corrosion of busbars and interconnect, cracks in the cell, shunt paths, damage of the glass and bypass diode failure, the back sealing, degradation of the antireflective coating, delamination between the glass encapsulant and the cell encapsulant surfaces and moisture-induced degradations [17,19-20, 23-26]. In a study conducted at the laboratory, four similar size PV backsheets layer are exposed at different times short wavelength region from 365 nm to 295 nm. According to test results, physical changes such as yellowing and aging have been observed [25]. Due to degradation, reaching light to the PV cell is reduced, thereby, output power of the module is dramatically reduced [27]. In addition, UV is found to change chemical structure in organic photovoltaic modules and therefore it caused a decrease in photocurrent at high photon energies [28]. PV module degradation does not depend only on external factors because degradation was observed about 12% on PV module even in the storage environment over the 30 years [20]. Energy efficiency is important, as well as it is extremely important to be able to observe and detect degradations in the PV modules. These can be conducted by visual inspection, digital image with UV light illumination, I-V curve analysis, IR thermography and EL imaging [17].

The snail trails are a kind of micro cracks cell on the modules. Figure 2 shows a PV module affected by the snail trail. Depending on snail trails, maximum generation of power can reduce up to 37%. Also, annual generation of power can be reduced up to 32% [29]. Not every micro-crack will be perceived as snail trails. However, if a PV module cell has a snail trail on the surface, then there are micro cracks [30]. Another study has been reported that PV modules affected by snail trails ranged between 68% and 88% [31]. Therefore, the snail trails on PV modules could be considered as a serious defect for the modules.

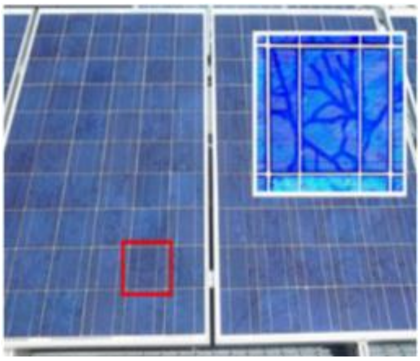

Figure 1.3. Visible picture of snail trail [29].

In this study, photovoltaic panel fault types and fault detection methods were investigated. Scenarios that contain fault types were created in simulation environment. Shading case, line to line fault, soiling problem that the annual losses caused by soiling between 3-6% and 14% [32], degradation: increase in resistance between module cell problem, bird droppings-tree leaves problem, and temperature impacts on PV module. All these scenarios can be encountered in PV systems.

In addition, hot spot heating problem caused by shading falling on the panel was investigated. To do this, an object is located on different surfaces of the panel. It was observed that it was different from the unshaded part of the PV module when compared to the signal output caused by the object placed on the surface. The output signal is received via the Arduino control card and transmitted in series to the Matlab program.

As an alternative to image processing with thermal imager which is one of the classical fault detection methods, UV detection has been developed. The user interface has been created with Matlab program. The surface of the photovoltaic panel was scanned and plotted on the screen. In the UV spectrum level (390nm-400nm), yellowing PV panel cells can be detected. Yellowing is one of the serious problems that may occur in PV panels that are exposed to radiation for a long time. It is formed with the formation of chromophores, which are portions of macromolecular chains that selectively absorb the different frequencies of visible light, giving colour to molecules [33]. In the interface developed with Matlab/Simulink program, it is observed that the signal output data of the yellowing region are different.

Also, it was observed in the laboratory environment, whether the cells, where the series connect on the PV panel were disconnected and glass surface fractured, could be detected in the infrared spectrum.

1.1 Literature Review

It is known that solar energy has been used since ancient times. For the first time, Socrates (BC 400) stated that the south side of the houses should have more windows to benefit from the sunshine. Archimedes (BC 250) burned the ships in Sirakuza by focusing solar radiation with concave mirrors. In 1725, Belidor developed a solar water-powered water pump. In 1839, a French scientist, Edmond Becquerel discovered photovoltaic effect of a solar cell, which is a basic physical process which generated power from sun. Improved solar photovoltaic cell was produced at Bell Labs in the United States in 1954. It was the first device to generate electricity from sunlight [34]. During the World War I, petroleum gained importance so the work toward solar energy has diminished. At the beginning of the 1960s, solar energy was understood as an alternative energy source in Turkey and relevant studies have started [35]. PV was successful in its early missions of powering the space satellites [36]. According to the International Energy Agency, global use of PV has been increasing since the 2000s with a 40% growth rate per year. Also it is stated that around 11% of global electricity generations will be provided by PV Plants until 2050 and it is corresponding to 4500 TWh per year [37]. With all these developments and expectations, an efficient real time monitoring and fault detection strategy is very important to detect faults in solar energy generation plants; thus, there are numerous studies about this in literature. Photovoltaics- based modules are widely used in industrial, commercial, and residential areas due to being a sustainable and environmentally based power source [38,39]. Due to the increasing popularity of PV-based energy, many studies have been conducted to increase the performance and reduce the cost of PV modules [40-42]. Despite a number of studies on PV performance have been carried out around the world, PV modules are still exposed to many external effects (partial shading, high temperature, irradiance fluctuation, accumulated dust, UV) that will decrease its efficiency [43,44]. Generally, the overall power output decreases between ~0.5% and ~0.05% for every 1°C increase in temperature [45]. In addition, the efficiency of the PV panel decreases based on the area covered by the shade. Besides, dust that is solid particles with diameters smaller than 500 μm is a critical parameter for the PV system due to a decrease in the efficiency of the modules. It occurs depending on different natural sources in the atmosphere and these particles could contain animal and human cells, sand, organic matters, clay, ash, etc. [46,47].

Abass et al. performed an experimental study to measure the effects of three types of construction materials pollutants (Cement, plaster and borax) on the efficiency of the PV modules. According to the result obtained by comparing clean and polluted modules, the efficiency of the panel was observed to decrease over 25.8% depending on the materials[48].

Adıguzel et al. proposed an Adaptive Neuro-Fuzzy Inference System (ANFIS) model for the prediction of dust particle size effect on the efficiency of PV modules. In this study, with the ratio of Root Mean Square Error (RMSE) as 0.18719, the ANFIS model has been quite successful in power estimation for PV modules [39].

Guo et al. examined the effect of dust and weather conditions on PV performance between June 1st - December 31st 2014 in Doha, Qatar. In this study, three PV array groups have been used. The first group called "high wash" was cleaned every week, the second group called “medium wash” was cleaned once in two months, and the last group called “low wash” was cleaned once in six months. Figure 1.4 shows that accumulated dust on the PV modulus causes a significant loss in the efficiency of the PV modules. A cleanness index (CI) is a performance ratio based on the cleannes and dustiness of the PV modules [49]. The CI could be calculated in 24-hours a day as follows:

$$CI = \frac{PR_{T\_corr}}{PR_{T\_corr\_clean}} \tag{1.1}$$

Where

PRT_corr is the temperature-corrected performance ratio of the PV module
PRT_corr_clean is the temperature-corrected performance ratio of a “clean” PV module.

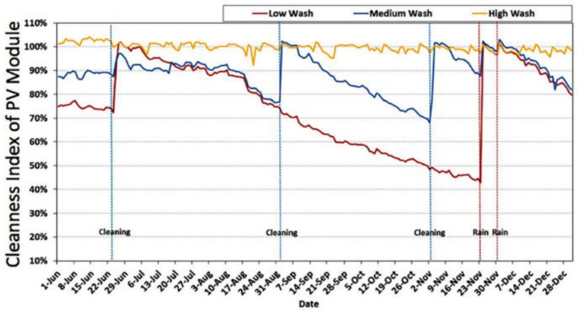

Figure 1.4. PV energy production decrease due to soiling [49].

Salimi et al. examined the effect of dust concentration on the PV surface. In this study, CI has been affected positively when measured with wind speed and affected negatively when measured with humidity and dust concentration. The performance of the PV module has been negatively affected by the accumulated dust between the ratio of 8–12% per month [50].

Chaichan and Kazem examined the effects of various cleaning materials (water, detergent, liquid soap, sodium detergent, etc.) on the panel efficiency. The results showed that the pollution-related power reduction rate decreased by 51%, 60.1%, and 68.4% with water, detergent, and liquid soap, respectively. However, it was observed that the most effective of them was sodium detergent with the reduction rates of 77.5% and 88.6% [51].

Kazem and Chaichan, analysed the chemical particles of dust accumulated on the PV module in different nine places depending on the distance from any industry and the traffic of the city and proposed a cleaning method. The result of the study showed that cleaning the PV module with water is sufficient for industrial and traffic-free locations. However, in places close to the industrial areas and traffic, it could be preferred to clean the PV modules with a sodium solution to reduce the effect of particulate matters (PM) [52].

Lu and Zhao examined the behaviour of different sizes of dust and the effect of wind speed on dust accumulation. This study also proposed a computational fluid dynamics simulation to predict the dust deposition effect on the PV output efficiency. The results showed that the ratio of accumulated dust has been increased first, and then decreased although the dust diameter increases. Figure 1.5 shows the effects of different sizes of dust at different speeds [53].

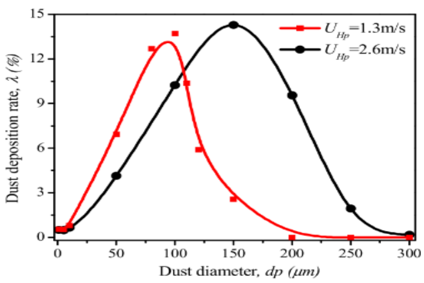

Figure 1.5. Dust deposition rates on PV panel[53].

In the study conducted by R. Hariharan, M. Chakkarapani, and G. Saravana Ilango, the PV plants could be categorized into two groups: model-based methods and history-based methods. The model-based method includes the comparison of real time data and simulations. In the other method, the data are collected first, and then machine learning and computational intelligent procedures are used for fault detection on the PV plants [54].

Kian Jazayeri carried out a study using artificial intelligence technology, and realized the intelligent fault detection system to detect shadows, damaged panels or cells, etc. based on the generated electric power by estimating the output power with according to the sun's position in the sky [36].

P. Jenithaa and A. Immanuel Selvakumar suggested that single fault current source is PV array because there is no utility inverter to produce overcurrent or overvoltage. Because there is no back feed current into PV array faults from utility grid, this consideration could be appropriate [55].

Radu Platon, Jacques Martel, Norris Woodruff, and Tak Y. Chau realized the fault detection and the principle of the comparison from the ac power production between the measured and model prediction [56].

Moath Alsafasfeh, Ikhlas Abdel-Qader, Bradley Bazuin, Qais Alsafasfeh and Wencong Su suggested performing a quick fault detection in the PV panel using thermal and CCD video camera mounted on drones [57].

Mohammed Tadj, Khalil Benmouiza, Ali Cheknane, Santiago Silvestre suggested a method to detect the occurrence of short-circuit failures in PV systems which used a fuzzy logic based approach [58].

Elyes Garoudja, Fouzi Harrou, Ying Sun, Kamel Kara, Aissa Chouder, Santiago Silvestre presented an innovative method that can detect thefaults on the DC side of PV panel according to the shading of PV modules. This method detects the incipient changes in a PV system [59].

Harun ÖZKISI and Murat TOPALOĞLU estimated the photovoltaic cell productivity in their study. Artificial Neural Network technics are used for it since it accurately estimates the productivity value of the PV cell as a percentage [60].

Akif KARAFIL, Harun OZBAY and Metin KESLER investigated the effect of temperature on the panel and observed that low temperature and high radiation increase the efficiency of the panel [61].

Tarak Salmi, Mounir Bouzguenda, Adel Gastli, and Ahmed Masmoudi developed a PV panel simulation and experiment at different physical and environmental conditions. Short circuit current, maximum power and open circuit voltage data from simulations and experiments show a good agreement [62].

In another study by M. Irwanto, Y. M. Irwan, I. Safwati, Wai-Zhe Leow N., cooling system was used to increase the PV panel efficiency, and the efficiency of the PV panel increased from 10.3% to 14% [45].

Ye Zhao performed a fault analysis in solar photovoltaic arrays. The study mentioned about the night-to-day transition fault because in the night there is no solar irradiance but during the sunrise, the PV panel voltage increases according to the solar irradiance. At that time, the inverter starts minimum voltage and MPPT starts to work. Then the PV system provides maximum power for the utility grid. This situation causes PV panel faults [63].

R. Hariharan, M. Chakkarapani, and G. Saravana Ilango conducted a study to detect the PV array faults and partial shading in the PV systems. This study also investigated the efficiency of the PV panel under different irradiation conditions[64].

The study by Mohammed Tadj, Khalil Benmouiza, Ali Cheknane, Santiago Silvestre presents a new method to detect the faults in the PV systems. It utilizes the satellite image for getting solar radiation data and calculating the generated power for detecting the failures [58].

Thesis Outlines

This thesis study has included five sections, which are explained by the following points:

1. Section 1: Represents an introduction to the works and studies about PV panels.

2. Section 2: A review of the photovoltaic system such as how PV modules works, which materials are used in PV system, what kinds of fault is encountered is given in this section. Additionally, PV fault detection techniques are given in this section.

3. Section 3: This section presents the mathematical model and simulation of PV modules. Besides, some PV panel faults scenarios have been implemented by Matlab/Simulink program. Simulation results are given in the figures.

4. Section 4: This section presents the material and method which are used in experimental studies.

5. Section 5: This section presents the conclusions and suggestions for future works.

2. REVIEW OF PHOTOVOLTAIC SYSTEM

2.1 Solar Cell Materials

In the solar cells, there are a lot of different semiconductor materials. Depending on the used materials in the cells, the efficiency and cost increase or decrease. Today, monocrystalline silicon, polycrystalline silicon, amorphous silicon, Cadmium telluride and copper indium selenide/sulfide are generally used for solar cells. A large amount of available solar cells is made from bulk materials. Their sizes are about 180-240 mm. Their processing is similar to the other semiconductor materials. Thin film layers, organic dyes and organic polymers materials are also available [36].

2.1.1 Crystalline Silicon

Crystalline silicon is the most popular material used in solar cells shown in Figure 2.1 The crystalline silicon solar cells are the first generation to produce electricity [65]. It has two important materials which are Silicon Wafers and Silicon Ribbons. The average energy conversion efficiency is about 12-18%, but the recorded efficiency for some laboratory is about 24.7% [66]. It has high production costs, but it has reliable and stable operation under environmental factors. According to crystallinity and crystal size, this material could be divided into categories like Monocrystalline Silicon (C-si), Polycrystalline Silicon or Multycrystalline Silicon (Poly –Si or mc-Si), Ribbon Silicon and Mono-like-multi-silicon [36]. The crystalline silicon has two types of photovoltaics which are used in the solar cells [67].

- Mono-crystalline silicon; Made by a high purity single crystal ingot.
- Multi-crystalline silicon; Firstly produced like a bar,then into wafers.

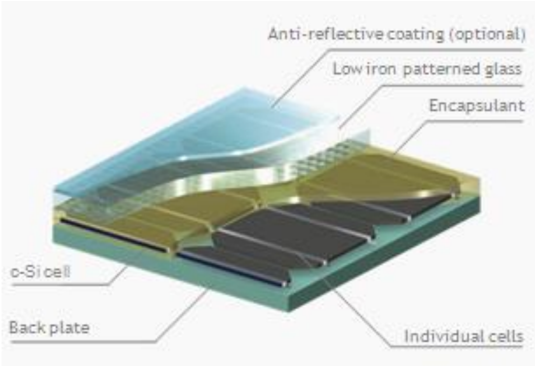

Figure 2.1. Crystalline silicon photovoltaics [65].

2.1.2 Thin Film Solar Cells

Thin film solar cells are heavier than crystalline cells and have lower efficiency that is shown in Figure 2.2. The thin film solar cells are the second generation to produce electricity [65]. When compared to crystalline silicon cells, it needs a larger area per watt production but the modules produce power at low cost per watt. When compared with crystalline silicon photovoltaics, thin film photovoltaic modules also have a relatively small drop in power output under partial shadowing. It is ideal to be used in large solar fields as well as in the Building Integrated Photovoltaic (BIPV) [68]. As the thin film solar cell Cadmium Telluride (CdTe), Copper Indium Gallium Selenide (CIGS) and Amorphous Silicon (A-Si) are generally used for outdoor solar power generation [36].

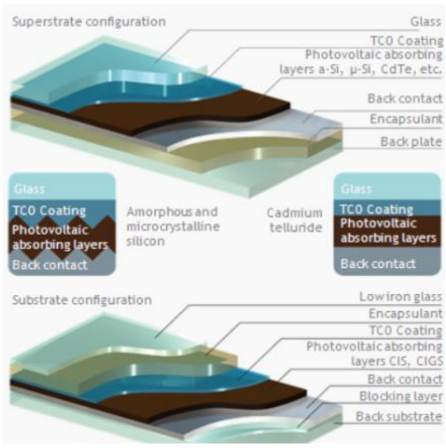

Figure 2.2. Thin film solar cells [65].

2.1.3 Other Solar Cell Technologies

Different types of solar cell are available in the market which are organic cells, dye-sensitized cells and light-concentration based GaAs cells. All of them, Organic Photovoltaics are the third generation to produce electricity [65]. It has higher defect tolerance when compared to many inorganic materials. Also it could easily be manufactured [69]. Organic Photovoltaics have lower efficiencies when compared to the second-generation solar cells, and it is illustrated in Figure 2.3 [65].

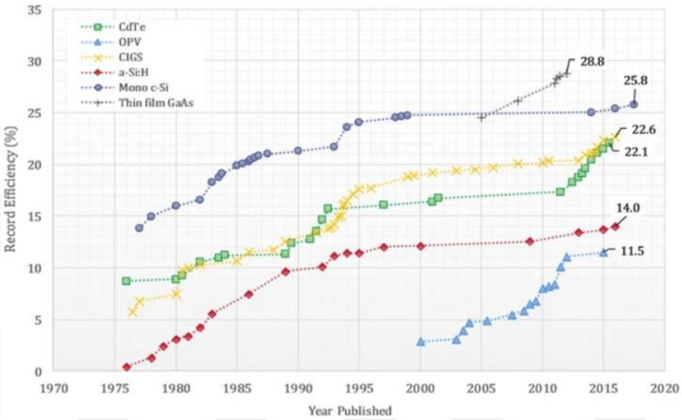

Figure 2.3. Comparison of the efficiency of solar cells [65].

2.2 Systems of Solar Panels

Nowadays, many applications are realized with photovoltaic (PV) modules in different areas such as buildings, aviation, solar power plants, land and sea transportations, etc [70]. Individual solar cells are used in calculators to provide power [63]. The PV module can be used vertically and horizontally to generate electricity. PV systems use solar cells to produce electricity depending primarily on the type and composition of the module, natural factor and also combined effect of the installation [71]. Solar energy is eco-friendly, renewable, clean and cost-free [57]. The solar photovoltaic system is one of the renewable energy systems which use the PV modules to convert sunlight into electricity. The PV plants used PV array to generate power for the utility grid [63]. Arrays consist of modules, and modules consist of cells. The solar cell, module and array are illustrated in Figure 2.4. The basic structures of a solar cell and a panel are illustrated in Figure 2.5.

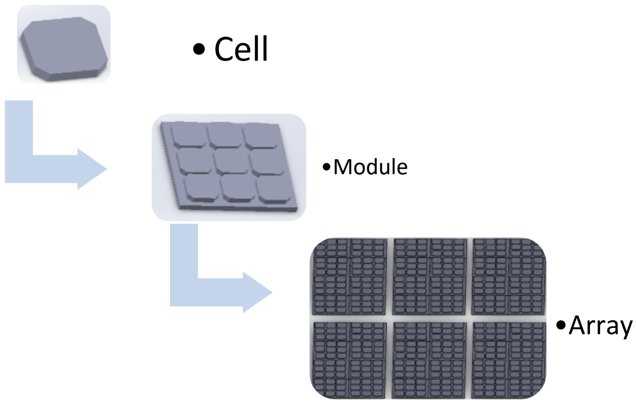

Figure 2.4. Illustrations of cell, module and array.

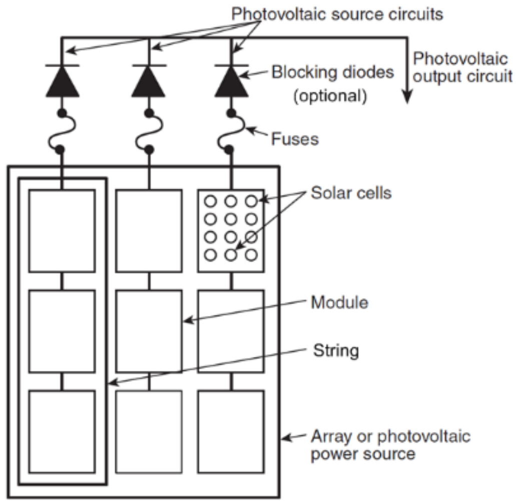

Figure 2.5. Block diagram of the Photovoltaic system [72].

2.3 How PV Works

Sun energy is the most abundant and freely available energy on planet earth. Without creating any water or air pollution, PV cells produce electricity from sunshine. There are at least two semi-conducting material layers in a typical silicon PV cell. The layers have positive and negative charges. There is an ultra-thin phosphorus doped (N-type) silicon in the positive charge layer. There is a thicker layer of boron-doped (P-type) silicon in the negative charge layer. P-N junction is the name where the two layers are closed [73]. The basic solar cell construction and panel are illustrated in Figure 2.6. When the cell is exposed to light, the electrons will gain photon energy and will be free to move. Some electrons from the N side will migrate to the P side and fill the existing hole there. Due to the electron migration, the N-side boundary becomes slightly positively charged and the P-side becomes negatively charged. An electric field is definitely formed between these charges. This electric field produces the necessary driving force. Electric current is produced due to this flow of electrons.

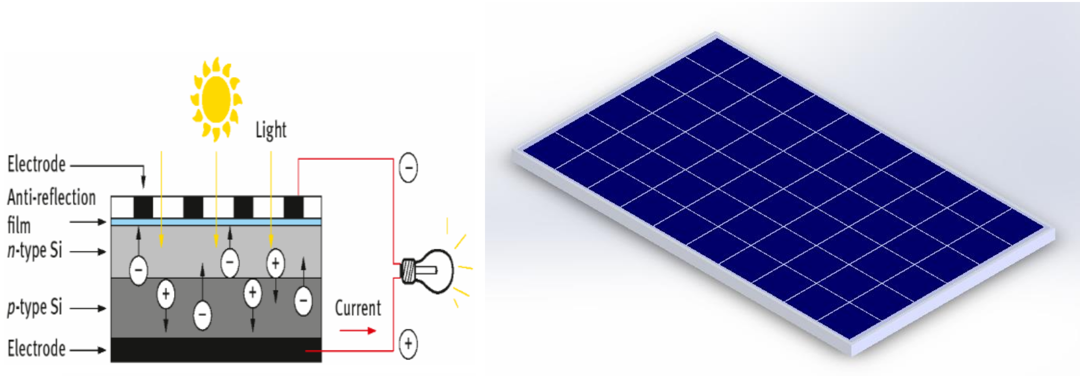

Figure 2.6. The basic structure of a solar cell[74] and panel.

Generally, there are two types of photovoltaic systems. They are classified depending on their operational and functional needs, component requirements, and how the energy is transferred to other electrical loads and electrical sources. These are grid-connected or utility-interactive systems and stand-alone systems [70]. There are six parts in the solar photovoltaic system. They are PV modules, solar charge controllers, inverters, battery banks, auxiliary energy sources and loads (appliances) [70].

• The PV module supplies electricity to the system.

• The solar charge controller regulates the voltage and current levels, and supplies energy to the battery. This prevents battery overcharging and prolongs the battery life.

• The inverter converts DC power into AC power.

• The battery is used to supply power when electric is needed.

• The load is an electrical appliance that is connected to the solar PV system such as laptop, washing machine, TV, etc.

• The auxiliary energy sources are diesel generators or other renewable energy sources.

Solar energy on the PV panel is converted to electrical energy with 6-20% efficiency depending on the semi-conductor material used in the PV panel. There have been many factors such as panel tilt angle, shading, dust, solar radiation level, temperature and the other losses that lead to low panel efficiency [36, 75]. Among these factors, the solar radiation level and temperature have been more prominent. When the PV modules absorb solar radiation, temperature of the modules increases, and this situation leads to a decrease in productivity. When the temperature of the PV modules increases, the efficiency of the PV module decreases about ~0.5%/°C and ~0.05%/°C [45]. In the PV modules, there are solar cells which are connected as series and generate an additive voltage. A PV module has a non-linear current vs. voltage (I-V) curve as shown in Figure 2.7. Short-circuit current (Isc), open-circuit voltage (Voc) and maximum power point (MPP) are three important points for the I-V curve. It provides maximum possible voltage, current and power, and it is related to a specific environmental condition [63] .

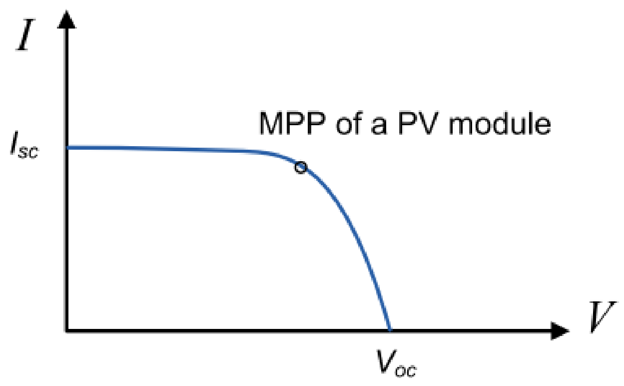

Figure 2.7. Illustrations of I-V curve of a PV module [63].

PV modules could be mounted in series and/or parallel to build a PV array. The entire PV module has an open-circuit voltage (Voc) and short-circuit current (Isc). Based on the connecting situation, the modules could take higher open-circuit voltage value and larger short-circuit current value. As seen in Figure 2.8, connecting m modules in series will yield a PV string with a higher open-circuit voltage (m×Voc).

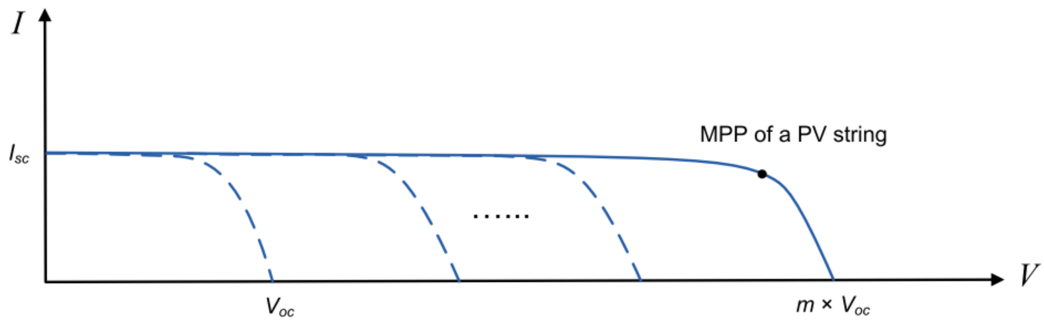

Figure 2.8. I-V curve of a PV string with m modules in series [63].

As seen in Figure 2.9, putting n strings in parallel will create a PV array with a larger short-circuit current (n×Isc).

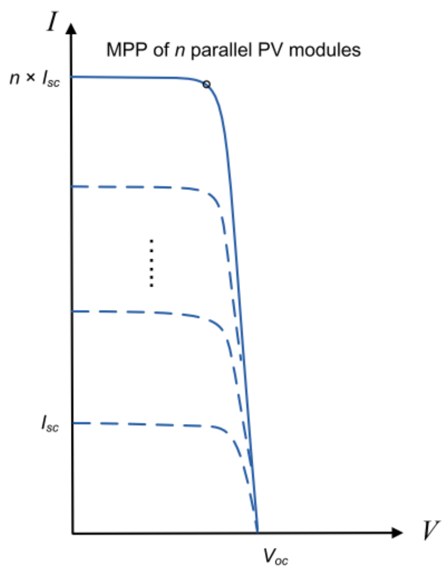

Figure2.9. I-V curve of a PV string with n modules in parallel [63].

To get more power from PV array, the topological methods shown in Figure 2.10 and could be used. If an array has m and n identical modules, it could be named as "n x m" PV modules. Thus, PV array generates higher power like that short-circuit current n × Isc and an open-circuit voltage m × Voc as seen in Figure 2.10.

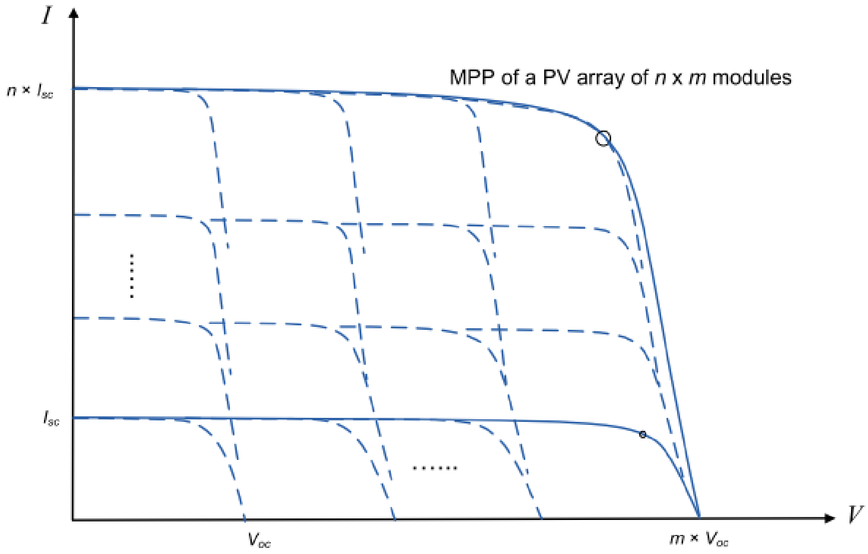

Figure 2.10. I-V curve of a PV array with comb. series and parallel [63].

2.4 Introduction to PV Faults

Power sum of the electrical outputs of individual PV modules creates total output power of the array. Predicted power is close to the normal operation power of the array. However, in some cases, many factors adversely affect the efficiency of PV array. Any condition that adversely affects the efficiency of the panels can be considered "fault" [76]. Faults in the PV system both reduces the electricity produced and affects the reliability of the whole system. Therefore, knowing the types of faults in the PV system is very important for maximum efficiency [34]. This may be a permanent or temporary fault. Generally, the causes of temporary faults may be bird droppings, shading and soiling or snow accumulation on the surface of the PV panel and the causes of permanent faults may be wiring losses, electrical disconnection and lifetime. When these two types of faults are compared, the temporary fault could be fixed in a short time, but the permanent fault could be fixed in a long time [76]. The classification of the most common types of faults in the PV system is illustrated in Figure 2.11.

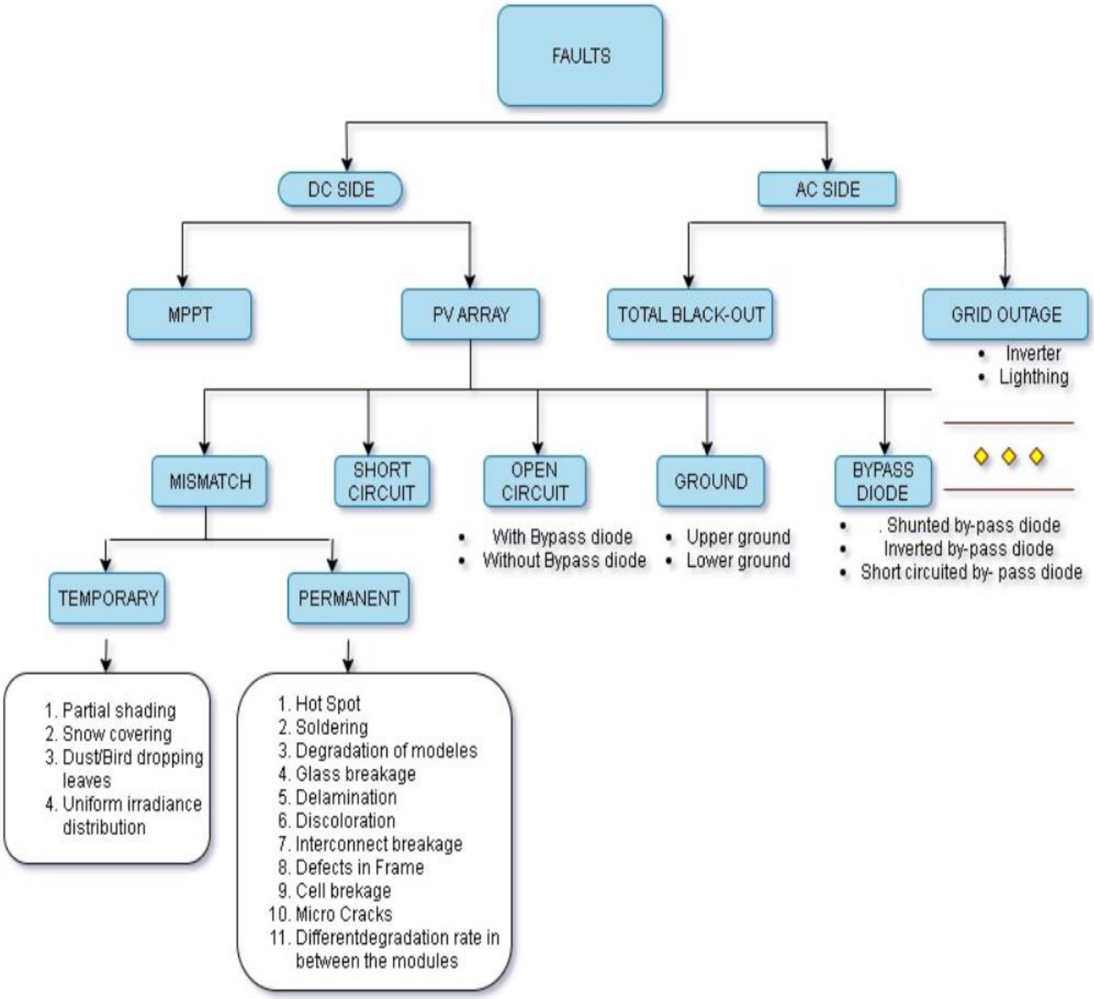

Figure 2.11. Classification of faults on PV system [76].

2.4.1 Hot spot fault

Hot-spot heating problems occur when there is one low current solar cell in a string of at least several high short-circuit current solar cells.

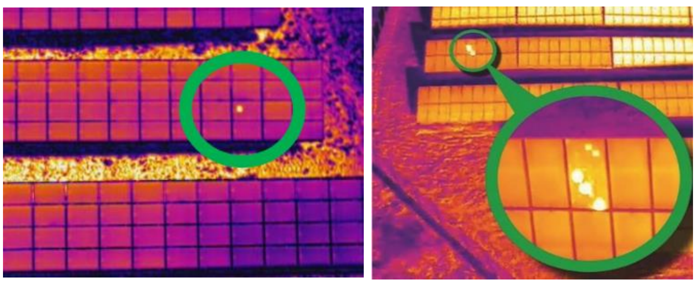

Figure 2.12 a)Hot spot fault, b)Multi hot spot fault [73].

It is the most common type of faults in PV panels. Therefore, computer simulation was performed for the reproduction of the behavior of Hot Spot Heating Problems using the Proteus 8.1 program.. There are 10 solar panel cells connected to each other in a series in Figure 2.13. All of the cells work in full efficiency (The current sources provide 1 amp power). There is no shaded cell which represents faulty.Total voltage generated from 10 cells is +8.34 V.

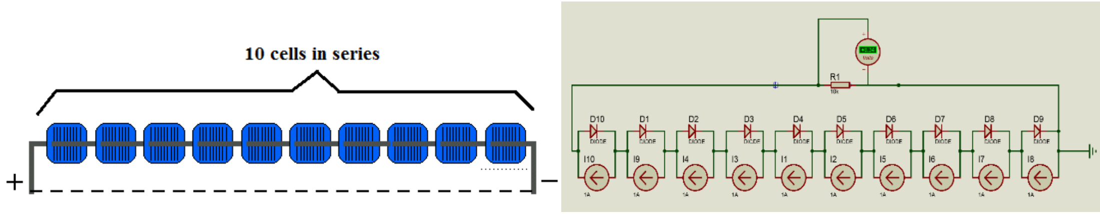

Figure 2.13. Full efficient series solar cells.

Although, inefficient series in the solar cells circuit is given in Figure 2.14, one cell is faulty that is shaded (The current sources provide 0 amp power). Total voltage generated from 10 cells is 0V. Also, when looked at the voltage on the last cell in Figure 3, negative voltage (-7.5 V) is observed. This is the reason for the undesirable Hot Spot Heating Problems in the panel.

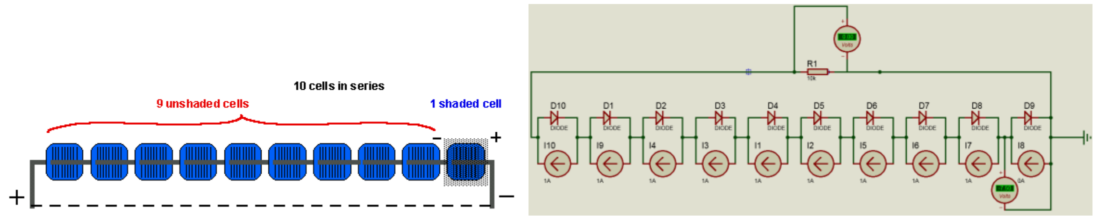

Figure 2.14. Inefficient series solar cells.

2.4.2 Diodes fault

Diode is designed to let current flow in one direction. There are two purposes of diodes in a PV system. One of them is Bypass diodes and the other one is Blocking diode, and they are illustrated in Figure 2.15 They have important roles in the protection of photovoltaic panels. The bypass diodes are used to reduce the power loss solar panels experience due to shading. The bypass diodes prevent each PV panel cell from reverse voltage damage while Blocking diodes prevent systems’ batteries from discharging backwards through panels at night.

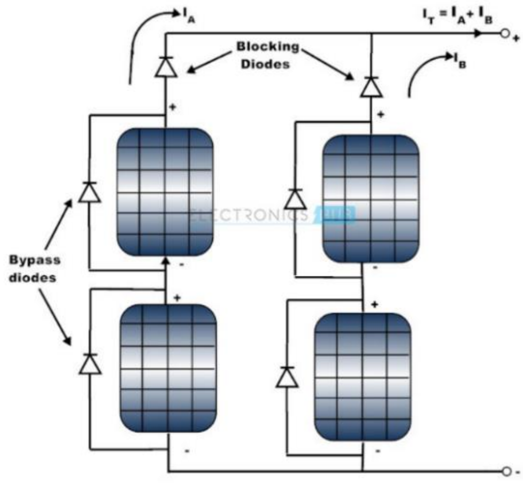

Figure 2.15. Bypass and Blocking diode [77].

2.4.3 Shading

There are two types of shading that are Subjective Shading and Objective Shading [78].Subjective shading is caused by objects that are near and far away because some layout of PV system is irregular. Therefore, sunlight could be blocked by a tree, building, soiling, etc. The Objective Shading is caused by heavy pollution and cloudy weather. These situations of the weather could block the sunlight. The efficiency of the PV array is affected by this shading because shading significantly reduces output power of the PV system. Because the amount of light reaching the panel is decreasing. Also, it may cause reverse voltage. [34]. A shaded PV system is shown in Figure 2.16.

Figure 2.16. Shaded PV system [79].

2.4.4 Snow cover

One of the most common reasons of faults is that the PV system is covered with snow, it is shown in Figure 2.17 because it causes energy losses. Even in the winter when the solar radiation is high, energy decreases are observed because the panels are covered in snow.

Figure 2.17. PV system is covered with snow.

2.4.5 Junction box fault

Junction box (JB) is located on the backside of the PV module- which is shown in Figure 2.18. Generally, there is a Block diode in the junction box and it provides protection from the PV module damage due to shadowing or hot spot. The reason for this failure may be moisture penetration, weak attachment of junction box, corrosion of connect point, poor wiring leading to internal arcing, poor mounting or thermal degradation [80].

Figure 2.18. Junction box [80].

2.4.6 Browning and yellowing fault

The uncontrolled chemical reaction causes browning or yellowing of the plastic materials on the panel which is shown in Figure 2.19.

Figure 2.19. Browning and Yellowing Fault [80].

2.4.7 Back sheet blistering

The reason for this is that the air and moisture find a way into the solar panel which is shown in Figure 2.20.

Figure 2.20. Back Sheet Blistering [80].

2.4.8 Delamination of a multicrystalline Si, c-Si and thin-film Module

Delamination occurs when the bond between the plastics (on the back) and the glass (on the front) separates. The reason for this is that the air and moisture find a way into the solar panel. Electrochemical corrosion effects are sometimes observed in the area of thin film PV modules on glass surfaces coated with tin oxide [81]. Delamination of the PV module is shown in Figure 2.21.

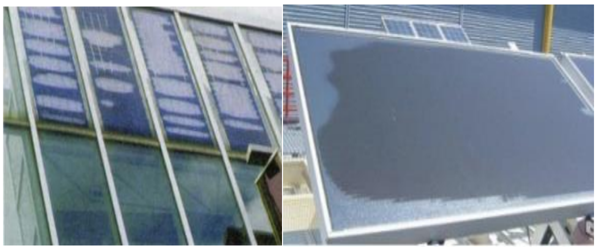

Figure 2.21. Delamination of PV module [80].

2.4.9 Glass breakage

Main failures of PV modules in the field seem to be from mechanical nature as glass breakage is shown in Figure 2.22.

Figure 2.22. Glass breakage [80],[79].

2.4.10 Burn marks at the backsheet

A higher local temperature on PV panel could reach hundreds of degrees Celsius, which can damage the backsheet [82]**.** It is shown in Figure 2.23.

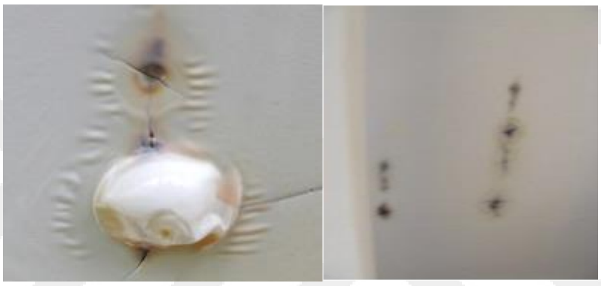

Figure 2.23. Burn marks at the backsheet.

2.4.11 Broken interconnection

The main reason for this failure is poor soldering of cell interconnect and string interconnect [83].Also, contraction or repeated mechanical stress and thermal expansion cause this [84]. It is shown in Figure 2.24.

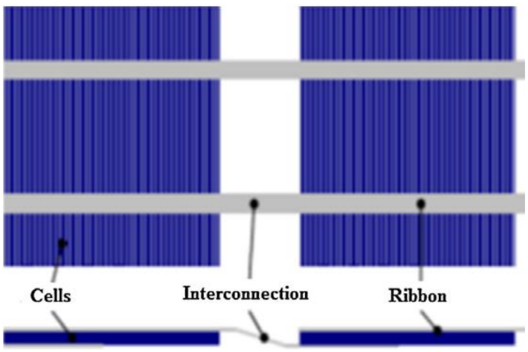

Figure 2.24. Broken interconnection PV system [85].

2.4.12 Cells cracking

One of the most common reasons of fault is cell cracking in the PV module. It could be encountered anytime. Manufacturing processor packing and shipping could be the reason for this. In addition, installation process could also be the reason for this fault [84,85].

2.5 Structure of PV System with Fault Detection and Diagnosis System

Figure 2.25 gives a general block diagram of the whole PV system which includes monitoring, fault detection, and diagnosis blocks. Solar energy conversion system consists of DC/AC converters with MPPT, PV array, and batteries. All of them is necessary for energy supply to grid.

There are two types of PV monitoring systems. One of them is ground-based system and the other one is space-based system. Sensors are necessary to measure the solar energy conversion system parameters in real-time in the ground-based system while there is no need for a sensor in the space-based system. Therefore, the space-based system is more economical. When comparing the ground-based system with the space-based system, the ground-based system is more reliable in terms of accuracy and it is not easily affected by climatic conditions [76].

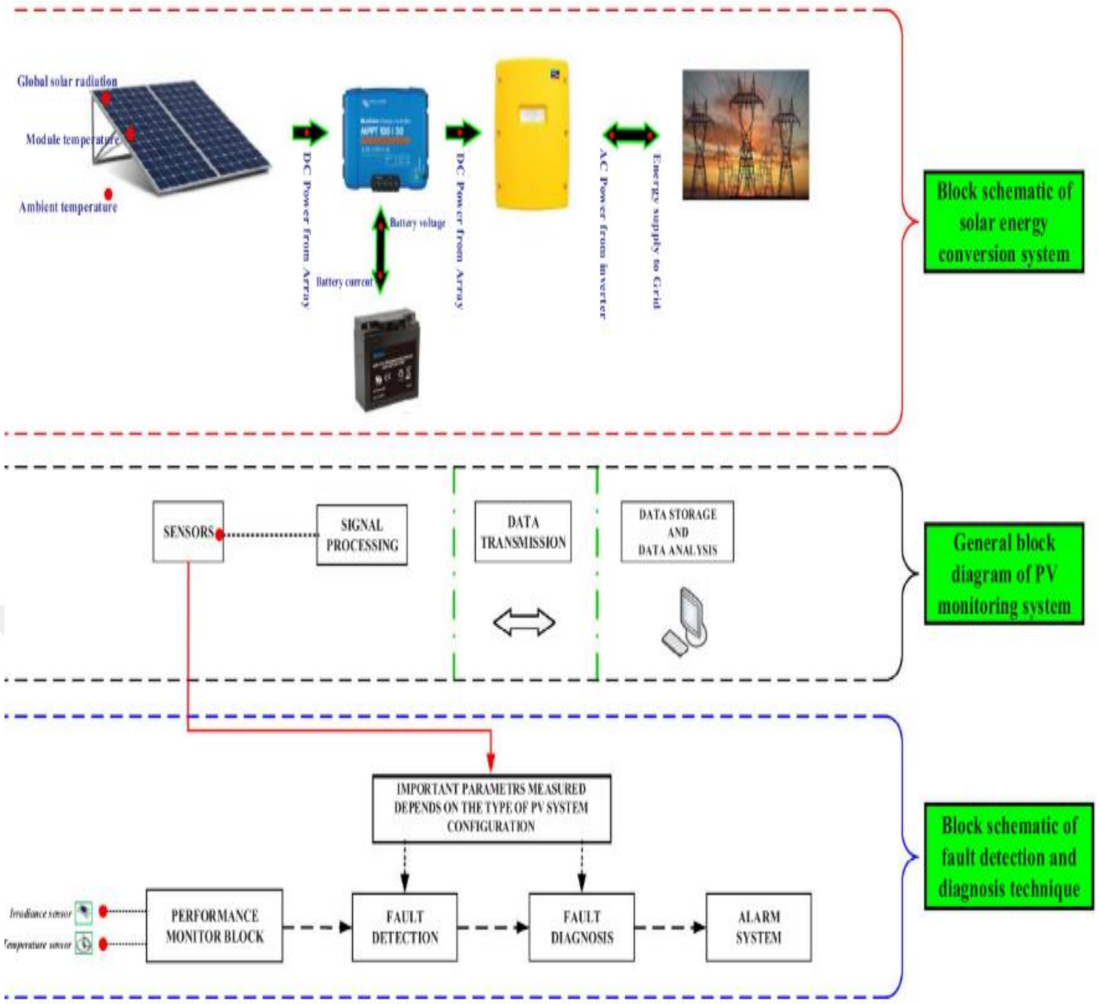

Figure 2.25. General block diagram of PV monitoring system [76].

2.6 PV Fault Detection Techniques

Fault detection in PV system is divided into two groups. One of them is DC group and the other is AC group. The DC group is located in the ground base system. It is divided into six groups such as: Electrical characterization, Infrared/Thermal imaging, Visual inspection, Ultrasonic inspection, Electroluminescence imaging and Lock in thermography. This study will focus more on this topic. There are numerous studies on the fault detection techniques in the literature. Quick detection of failure, required data inputs (electrical data and climatic) and selectivity (i.e., ability to distinguish between different faults) are the main features of such techniques. The fault detection methods in the literature were tabulated in Table 2.1.

Table 2.1. Analysis and classification of fault detection methods in literature.

Author	Ref.	Fault	Fault detection method	Validation	
				Simulation	Experimantel
Fadhel S.	[68]	partial shading	Real electrical measurements	✓	✓
Masoud A.	[86]	• Single phase to ground fault, • Phase to phase to ground fault, • Three phase to ground fault, • Phase to phase fault	discrete wavelet transform with multi-resolution singular spectrum entropy	✓	✓
Chaibi Y.	[87]	• short/open circuit failures, • inverter disconnection, • partial shading	Real electrical measurements	✓	✓
Yilmaz M.	[88]	– (effects of operating conditions)	Artificial Neural Network (ANN)	✓	✓
Navid K.	[89]	– (effects of operating conditions)	–	✓	✓
Dhimish M.	[90]	partial shading	Artificial Neural Network (ANN), Fuzzy Logic	✓	✓
Michal O.	[91]	short-circuit failure, open-circuit failure	Real electrical measurements	–	✓
Toufik S.	[92]	partial shading	Real electrical measurements	✓	✓
Siva R.	[93]	• open circuit faults, • line-line faults, • partial shading, with and with-out bypass diode faults	k- nearest neighbors (kNN)	–	✓

Table 2.1 (continue). Analysis and classification of fault detection methods in literature.

Author	Ref.	Fault	Fault detection method	Validation	
				Simulation	Experimantel
Moath A.	[57]	partial shading	real time inspection with thermal and Charge-Coupled Device CCD camera	–	✓
Coşgun A.E.	[70]	open circuit faults	Offline inspection with thermal camera	–	✓
Milan B.	[94]	Heating of the panels(weather conditions)	Real electrical measurements	✓	✓
Elibol E.	[95]	Heating of the panels (weather conditions)	Real electrical measurements	–	✓
Fermín M.	[96]	–	fault detection algorithm(comparison of simulated and measured productions)	–	✓
Wang Y.	[97]	partial shading	comparison of PV system normal and fault	–	✓
Fouzi H.	[98]	–	cumulative sum (CUSUM) chart efficiency	✓	–
Jenitha P.	[55]	• Open circuit faults, • Line-line fault with a small voltage difference Degradation fault	comparison of PV system normal and fault	✓	–
Sofiane K.	[99]	• Partial shadow, • Inverter disconnection	comparison of PV system normal and fault	✓	–
Dhimish M.	[100]	Partial shadow	Fuzzy Logic	✓	✓

3. MODELING AND SIMULATION OF PV MODULES

3.1 One Diode Model of PV Panel

The I-V characteristic of the solar cells is not linear. Therefore, their simple model is not appropriate as a constant current source or a constant voltage source. In the literature, two different type model are used to describe the electrical behaviours of solar cells [101,102]. The equivalent circuits for the one-diode model and the double-diode model are shown in Figure 3.1 and Figure 3.2.

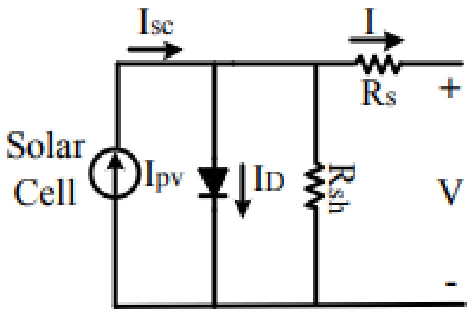

Figure 3.1. Equivalent circuits for the one-diode model.

For the one-diode model in Figure 3.1, the solar cell current equation is as follows (3.1):

$$I = I_L - \underbrace{I_{S1}\left[\exp\left(\frac{V + IR_{c,s}}{AkT}q\right) - 1\right]}_{I_{D1}} - \underbrace{\frac{V + IR_{c,s}}{R_{c,sh}}}_{I_{sh}} \tag{3.1}$$

Ipv is the current produced by the charge light, I_D diode current, I_{S1}, reverse saturation of the diode or leakage current, Ir, current through parallel resistance, q, electron charge (1.6X10-19 oC), k Boltzmann constant (1 , 38X10-23 J / K), T is the temperature at Kelvin of the pn junction, and α is the correction factor ranging from 1.0 to 1.5. Equation 3.1 shows the law of a basic Kirchhoff. The current produced by the module from the light is linearly connected to solar radiation and is also affected by temperature relative to equation 3.2.

$$I_{PV} = [I_{sc} + K_i\,(\mathrm{T} - T_n)]\,\frac{G}{G_n} \tag{3.2}$$

K_i is the short circuit current / temperature coefficient, sunlight in terms of G, W / m^2 and Gn is the nominal solar radiation value in W / m^2.

3.2 Double-diode Model of PV Panel

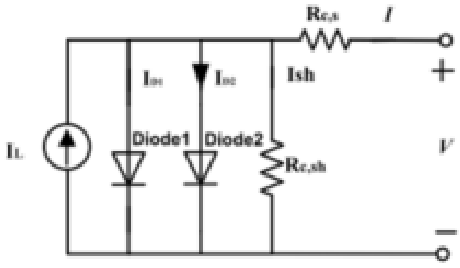

Figure 3.2. Equivalent circuits for the double-diode model.

For the double-diode model, the solar cell current equation is as follows (3.3):

$$I = I_L - \underbrace{I_{S1}\left[\exp\left(\frac{V + IR_{c,s}}{kT}q\right) - 1\right]}_{I_{D1}} - \underbrace{I_{S2}\left[\exp\left(\frac{V + IR_{c,s}}{2kT}q\right) - 1\right]}_{I_{D2}} - \underbrace{\frac{V + IR_{c,s}}{R_{c,sh}}}_{I_{sh}} \tag{3.3}$$

3.3 Simulation of PV Module with Matlab SIMULINK

The MATLAB/Simulink model of PV cell is shown in Figure 3.3. In this simulation, there are two inputs which are Temperature and Irradiation. Depending on these inputs, Output voltage, PV cell current and Power of the cell have been obtained.

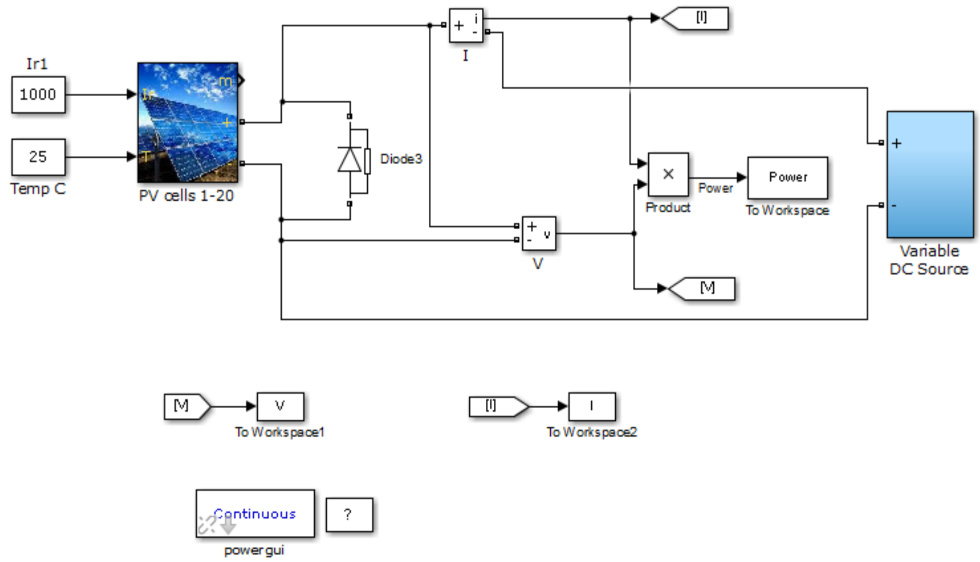

Figure 3.3. The MATLAB/Simulink model of a PV cell.

To understand the performance of the PV panel, a model simulation was created in Matlab/Simulink, and the following results have been obtained. It is obvious that the simulation results match the actual panel values. Figure 3.4 shows the 40 watt solar module electircal characteristics.

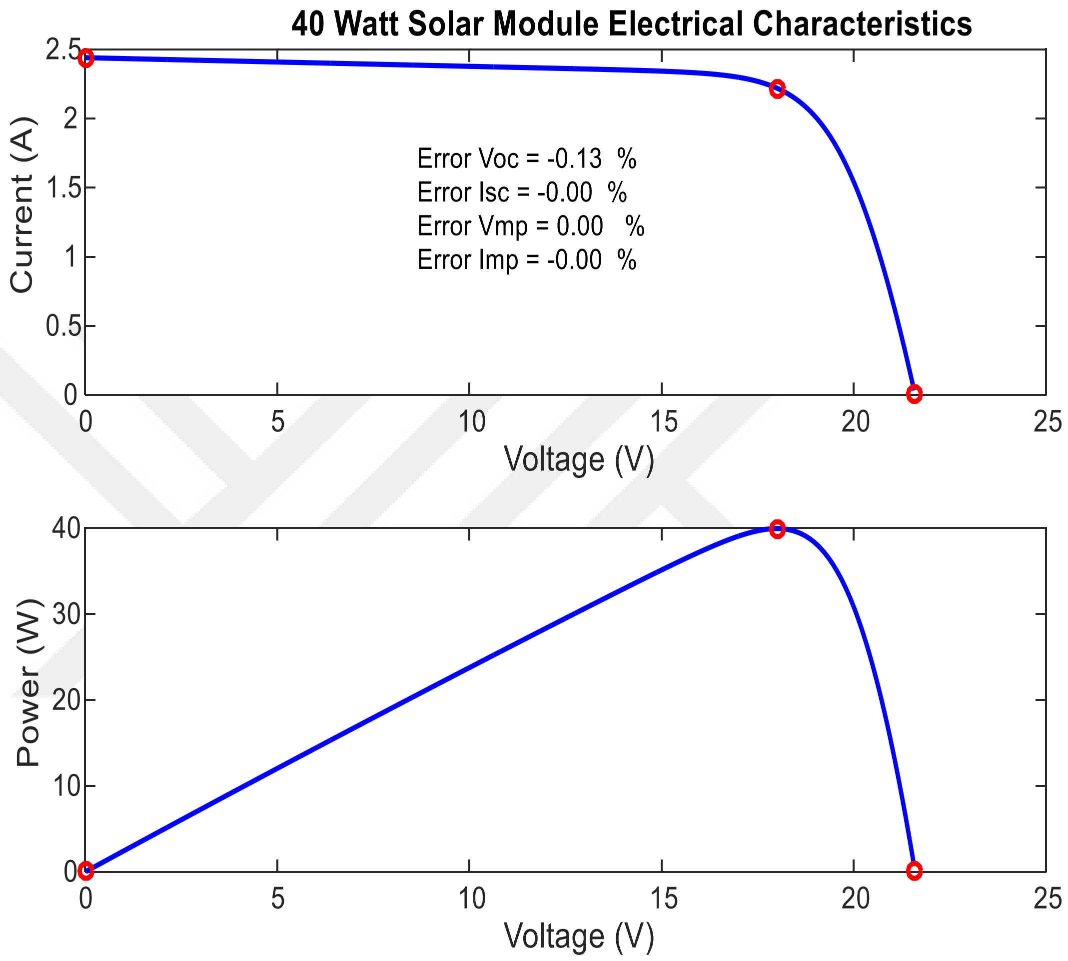

Figure 3.4. The MATLAB/Simulink model results of a PV cell.

The photocurrent changed due to shading. I_{ph} is the photocurrent generated by shaded PV cells as shown in the following (3.3) equation.

$$I_{ph} = I_{phs}\boldsymbol{\beta}\frac{S}{S_r} \tag{3.3}$$

Where I_{phs} is the photocurrent under the standard condition (Sr=1000 Watt/m2, Tr=25 °C) (Amperes); Sr represents the reference solar radiation (Watt/m2), Sr = 1000 Watt/m2; S is the solar irradiation (Watt/m2), and $\boldsymbol{\beta}$ is the shadow's transmittance.

There is a linear relationship between PV panel's output power and solar irradiation. Figure 3.5 shows the P-V curves of the PV model at constant temperature (25 °C) and under different irradiation. Depending on different solar irradiations, the highest points on the curves show the maximum power output. Maximum output power varies depending on the solar radiation level.

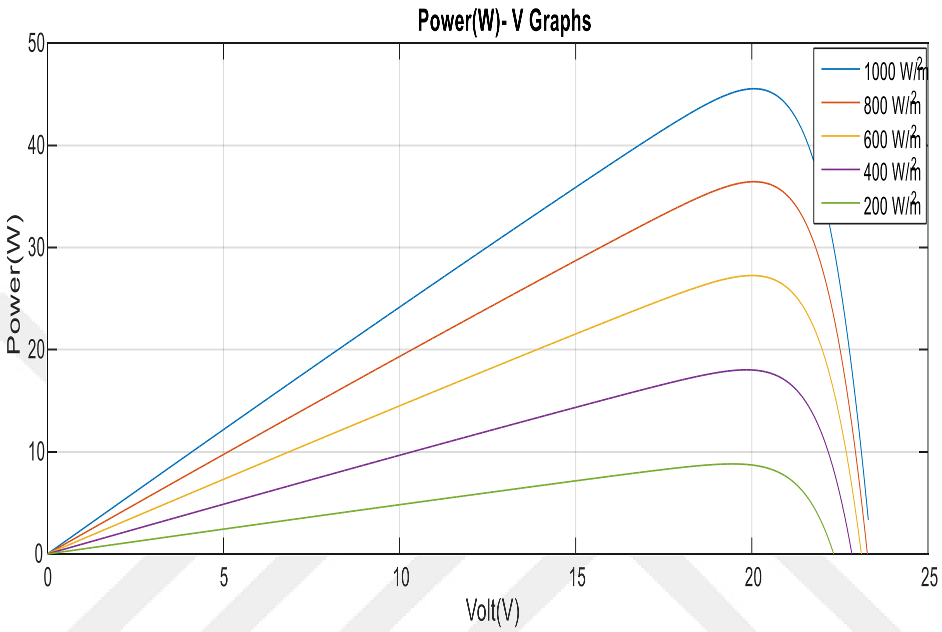

Figure 3.5. Simulation results (P-V) at different irradiation.

Figure 3.6 illustrates the current-voltage (I-V) characteristics of a typical silicon PV cell operating under different solar irradiations. When the voltage of the PV panel is at the maximum value, the current is at minimum. This is known as "solar cell open-circuit voltage" or "Voc." On the contrary, the current value is at the maximum point while the voltage is at the minimum point. This is known as "the solar cells short circuit current" or "Isc". The interval of the solar cell I-V characteristics curve changes from the short circuit current (Isc) at zero output volts, to zero current at the full open circuit voltage (Voc).

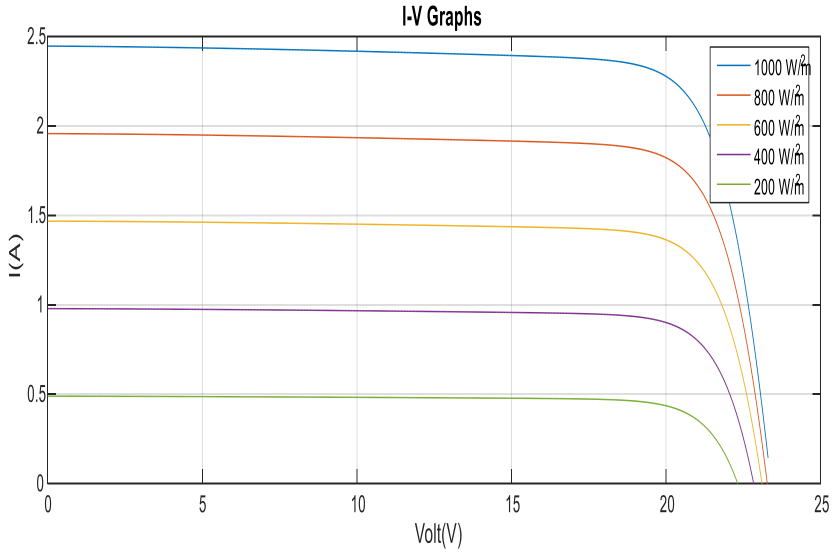

Figure 3.6. Simulation results (I-V) at different irradiation.

Semiconductors are very sensitive to temperature and are used in the production of PV panels. Figure3.7 illustrates the power-voltage (P-V) characteristics of a typical silicon PV cell operating under different temperature. It is clear that the decrease in the maximum output power point and open voltage is due to a rise in temperature. The PV gets power from a solar cell's product of current and voltage (I x V). If multiplication for all voltages from short-circuit to open-circuit conditions is done at all points, the power curve given in Figure 3.8 is obtained for a certain level of radiation.

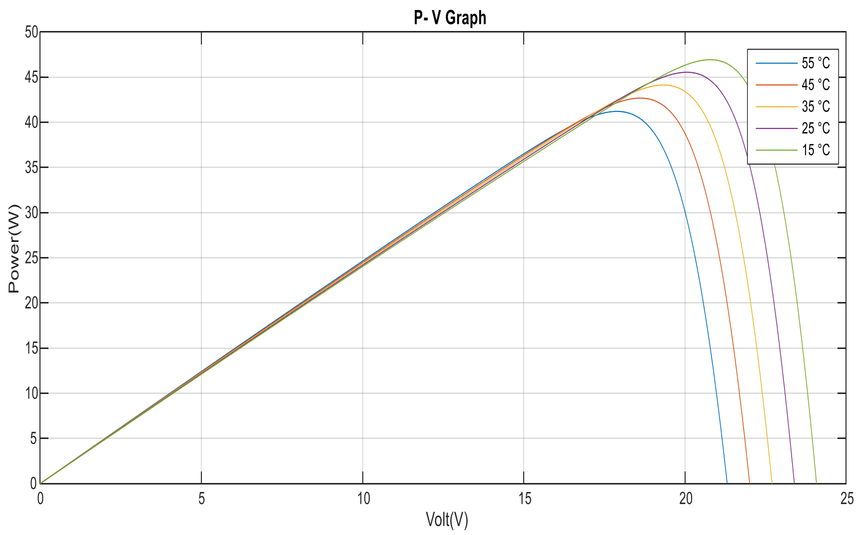

Figure 3.7. Simulation results (P-V) at different temperature.

The short circuit current slightly rises as the cell temperature increases while open voltage decreases more significantly.

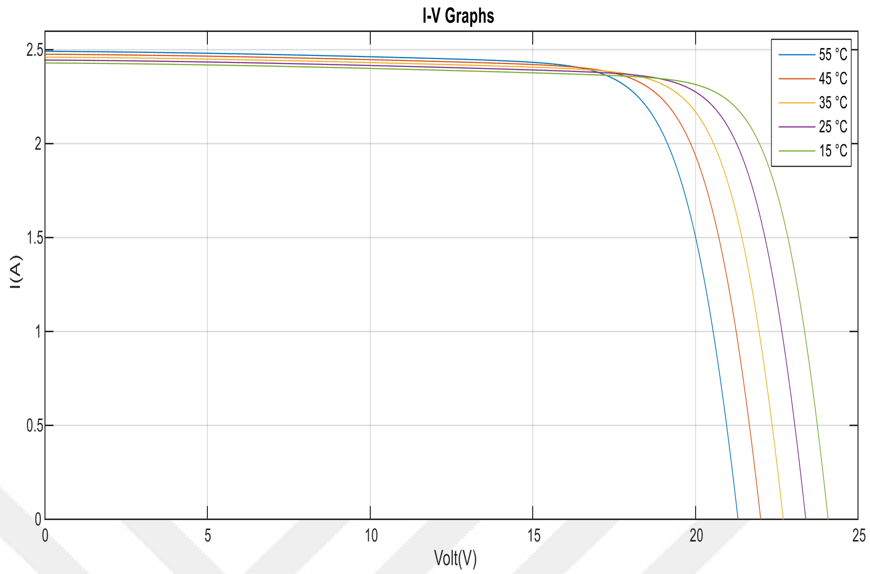

Figure 3.8. Simulation results (I-V) at different temperature.

The proposed diode model (illustrated in Figure 3.1 and Figure 3.2) can be easily simulated with the simulation programs such as PSpice or Proteus. They can also be simulated in MATLAB/Simulink accurately. The MATLAB/Simulink simulation program was used to observe I-V and P-V characteristics of the PV module in Figure 3.9.

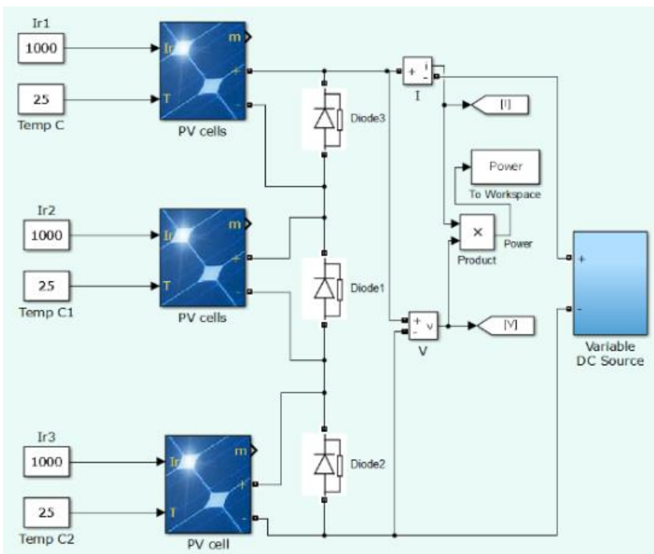

Figure 3.9. Simulation model for PV modules in MATLAB/Simulink.

To initialize the simulation, the operating parameters of modules obtained from PV's datasheet. Isc, Is0, Voc, A, Ir (irradiance levels) and T (standard test condition 25 °C) parameters set as constants in the Simulink model. The model consists of three series 40W PV cells. Each of them has Bypass diode to protect from reverse voltage. The power output of the normally operating PV system is obtained. The simulation results are available in Figure 3.10. When the simulation result is examined, actual operation data of the panel were observed.

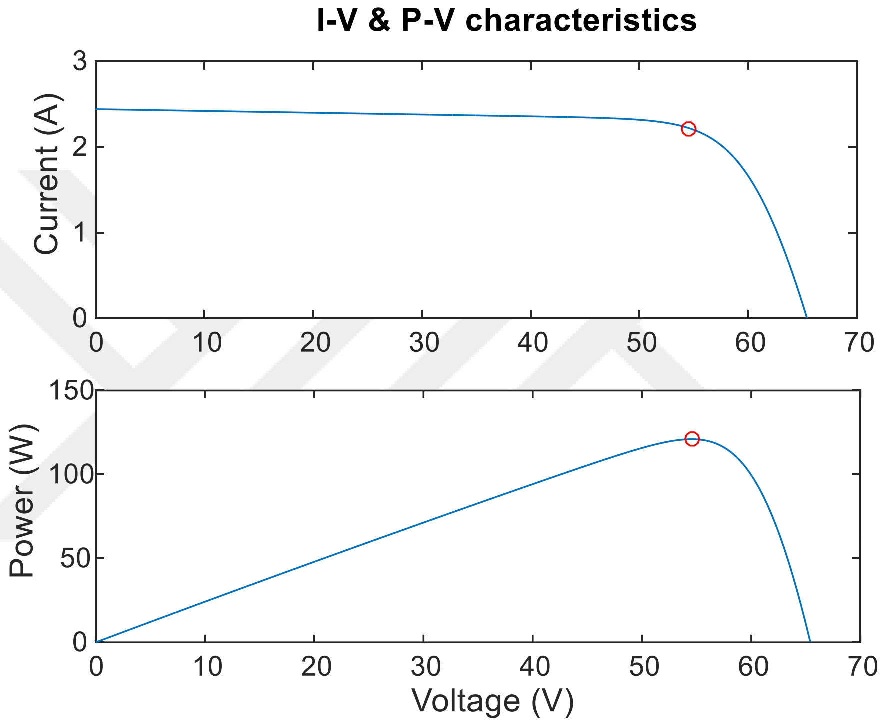

Figure 3.10. I-V and P-V characteristics of panel.

Also, using this Simulink model, some fault simulations of PV modules' scenario were performed. These are;

- Shading Fault,
- Line to Line Fault
- Snow Cover
- Temperature Effects
- Soiling
- Degradation: Increase in Resistance
- Bird Droppings or Tree Leaves

3.3.1 Shading case

Three identical PV modules connect to each other in the series. Each module generates 40 Watt output power under uniform insolation of 1000 Watt/m2 and surface temperature of the solar cell 25 °C. In case 1, just one PV module is shaded insolation of 600 Watt/m2 and the other two PV modules without shading (1000 Watt/m2). In case 2, two PV module is shaded insolation of 600 Watt/m2 and the other PV module without shading (1000 Watt/m2). Shaded PV module is indicated in grey colour and unshaded module is indicated in white colour. Case1, Case2 and their I–V and P–V characteristics graphs are shown in Figure 3.11. As a result, it is obtained that the output power generated by the shaded PV module decreases considerably when the two cases are compared.

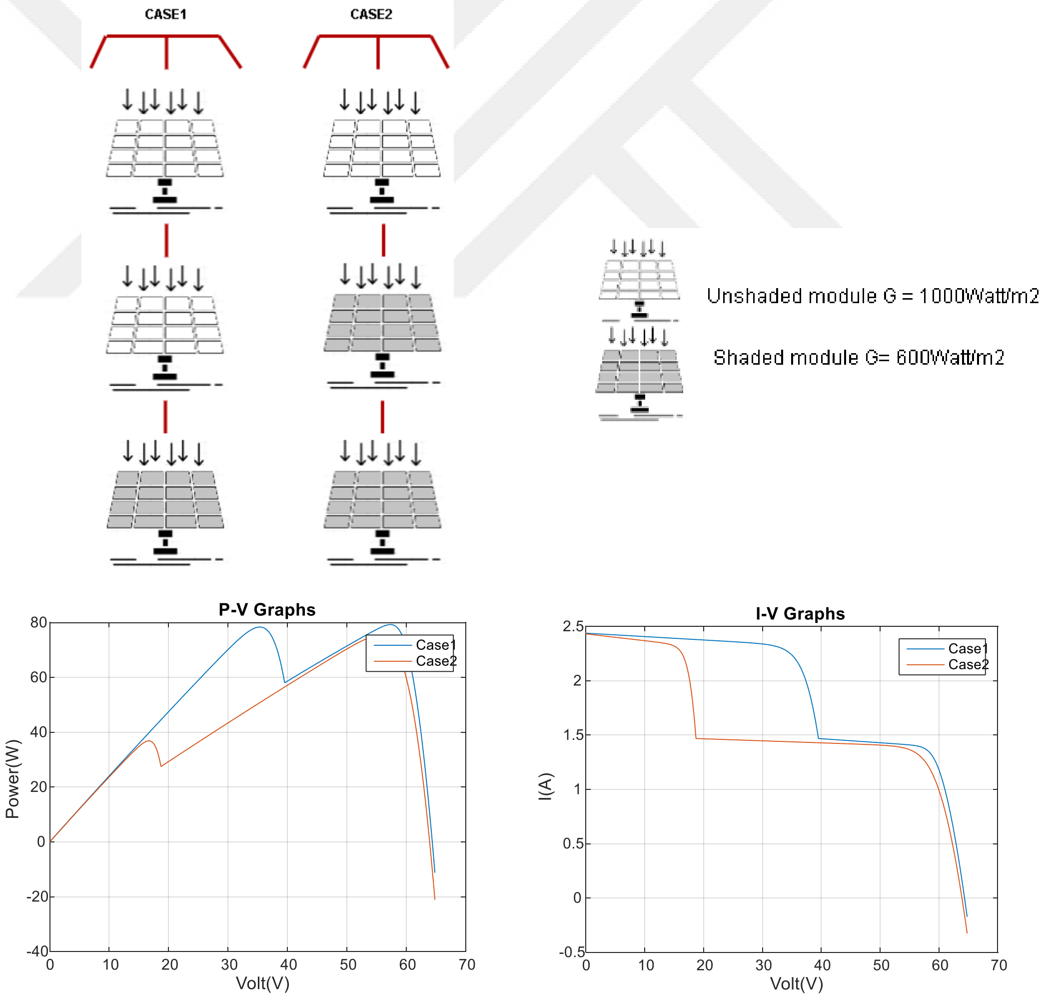

Figure 3.11. The PV modules configuration and graphs for shading

3.3.2 Line to line fault.

In Case 1, there two normal modules and one short circuit module. In Case 2, there are one normal module and two short circuit modules. It can be observed that all parameters generated by PV modules are affected. In Case1, the PV system can generate about 44-volt output while in Case2, PV system can only generate about 22-volt output voltage. It is shown in Figure 3.12.

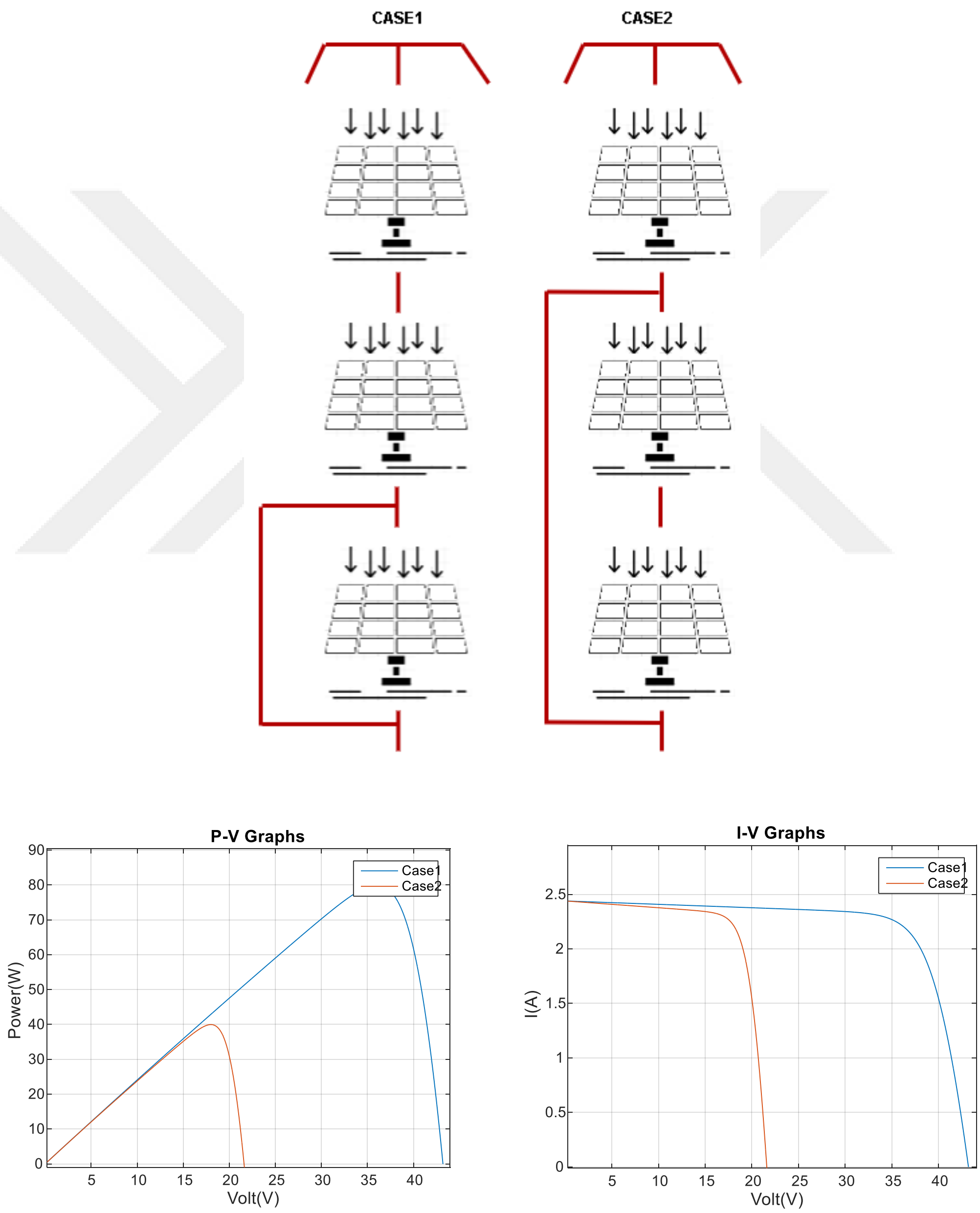

Figure 3.12. The PV array configuration for line-to-line fault.

3.3.3 Snow cover

In Case1, there are normal modules and in Case 2, there are snow cover modules. When two cases are compared, snow covered PV modules only receive 10% solar radiation while the other one receives 100% solar radiation [34]. MATLAB/Simulink models of the PV system that is covered with snow are developed to investigate their characteristics. The identical PV array module is also used in this case. In case 1, all PV modules have 1000 Watt/m2 irradiation while in case 2, all PV modules have 100 Watt/m2. It is obtained from this simulation that in Case 2, generated Power, Voltage and Current values decreased dramatically. It is shown in Figure 3.13.

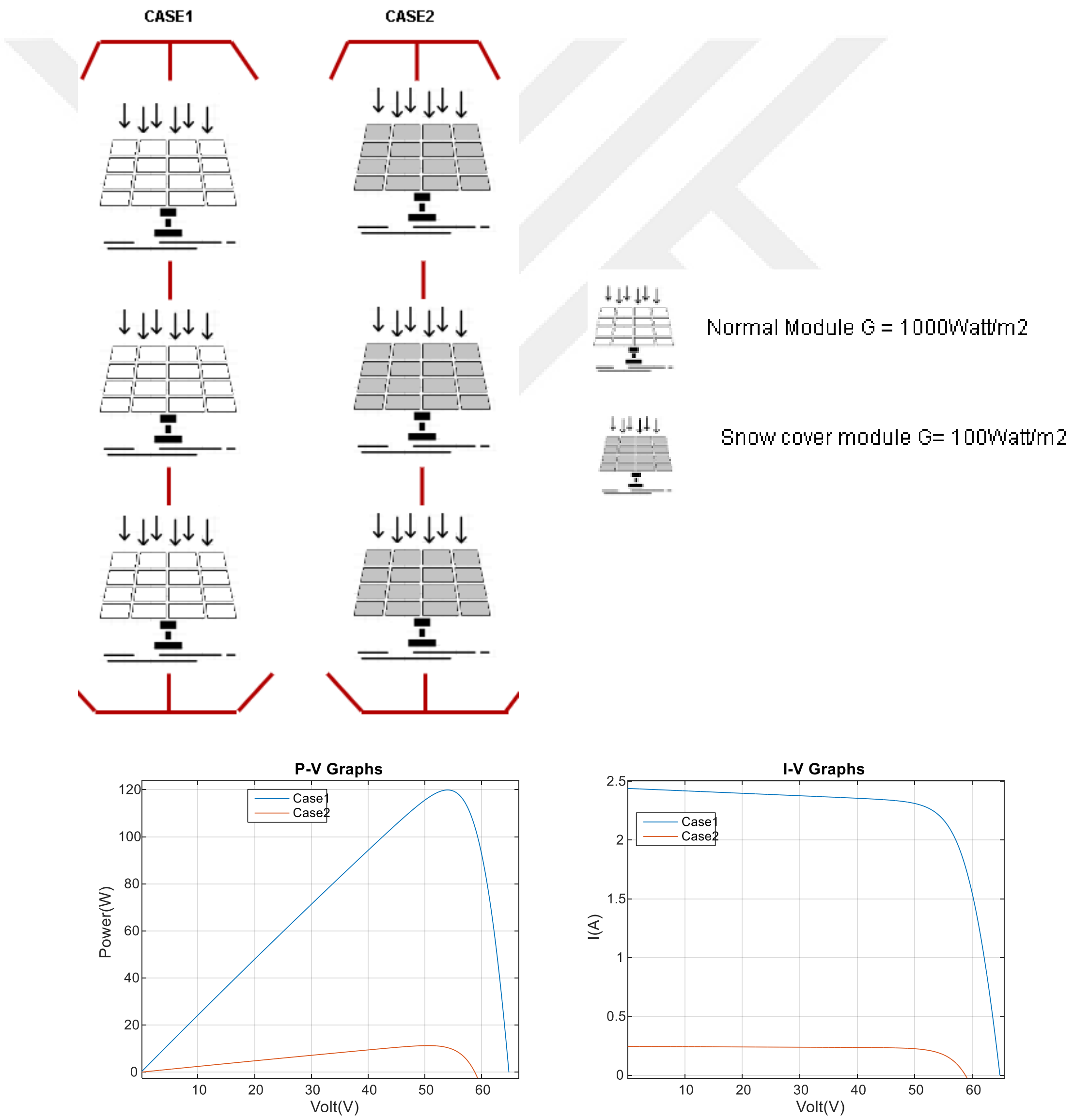

Figure 3.13. The PV array configuration for snow cover.

3.3.4 Soiling

If periodic cleaning of PV panels is not done, contamination on the panel will have a negative effect on the panel efficiency. This problem is also observed in places where rainfall is limited. In Case 1, all modules are clean and having 1000 Watt/m2 irradiation while in case 2, all PV modules have 950 Watt/m2 irradiation. It is beneficial in reference [34] for doing this assumption. In MATLAB/Simulink models, it has been observed that soiling has an effect on the PV system's generated power. It is shown in Figure 3.14.

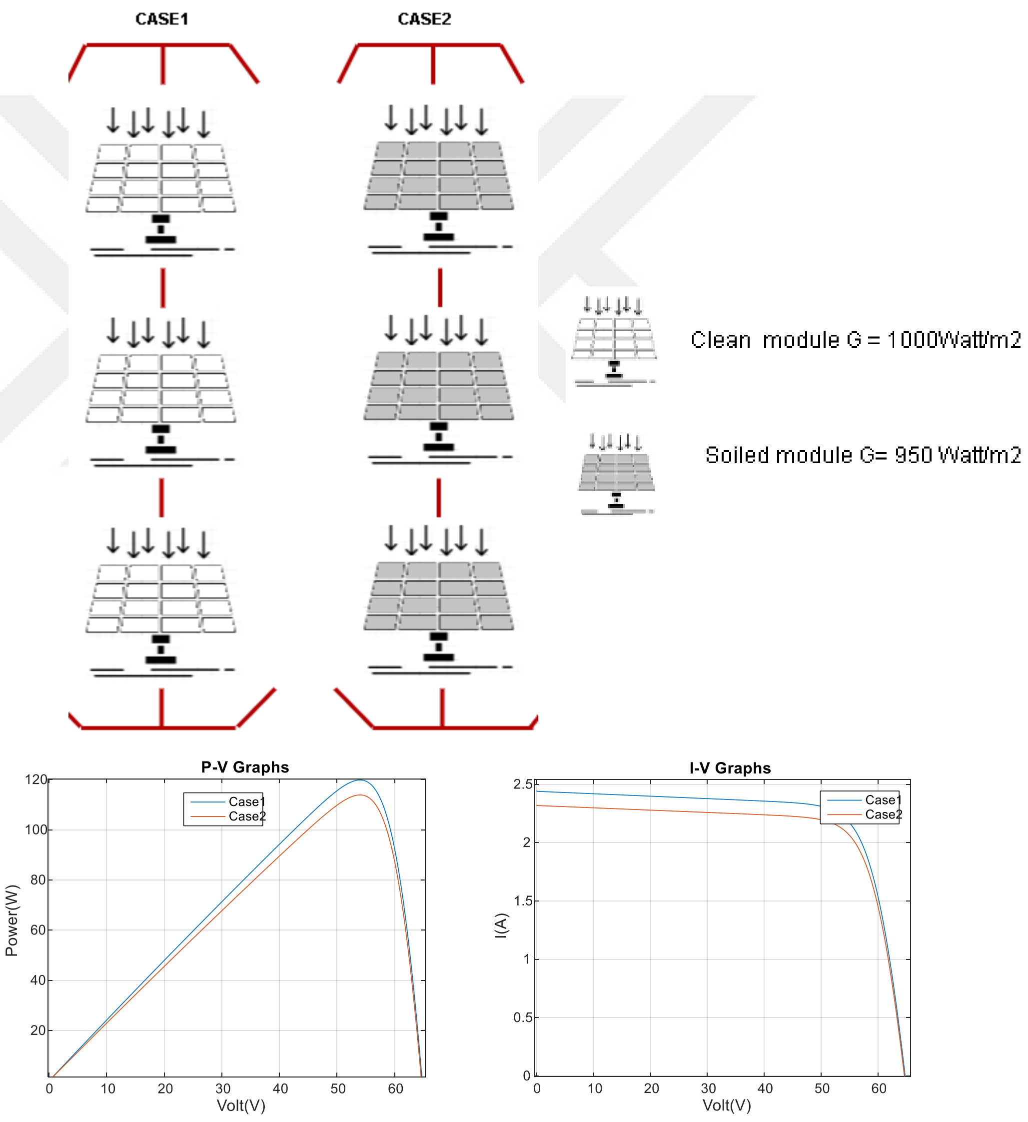

Figure 3.14. Soiling effect.

3.3.5 Degradation: increase in resistance

There are some graphs in Figure 3.15. Blue graph is representing normal modules' power output. Yellow and orange graphs are representing the decreased power output. Reason for this is resistance between the modules. Corrosion and decreased adherence of contacts occurs due to water vapours. This could be a reason for the increase in the resistance between the modules. Simulation of this situation was performed in Matlab/Simulink. It was obtained from this simulation that generated Power of PV panel values decreased dramatically.

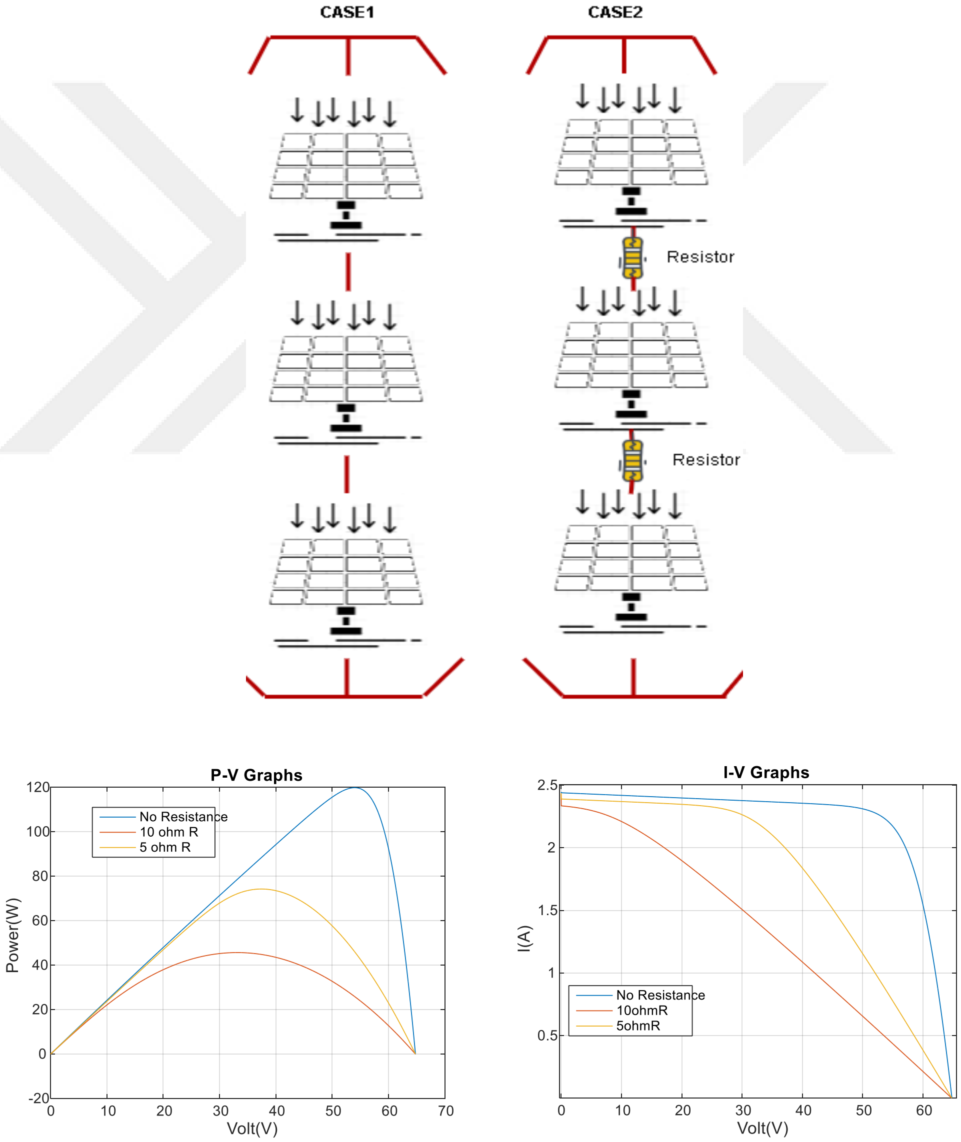

Figure 3.15. The PV array configuration for resistance between modules.

3.3.6 Bird droppings, tree leaves

Bird droppings and tree leaves can block light from reaching on the cells. The module cannot generate any output power if sufficient cells are fully covered. It is shown in Figure 3.16.

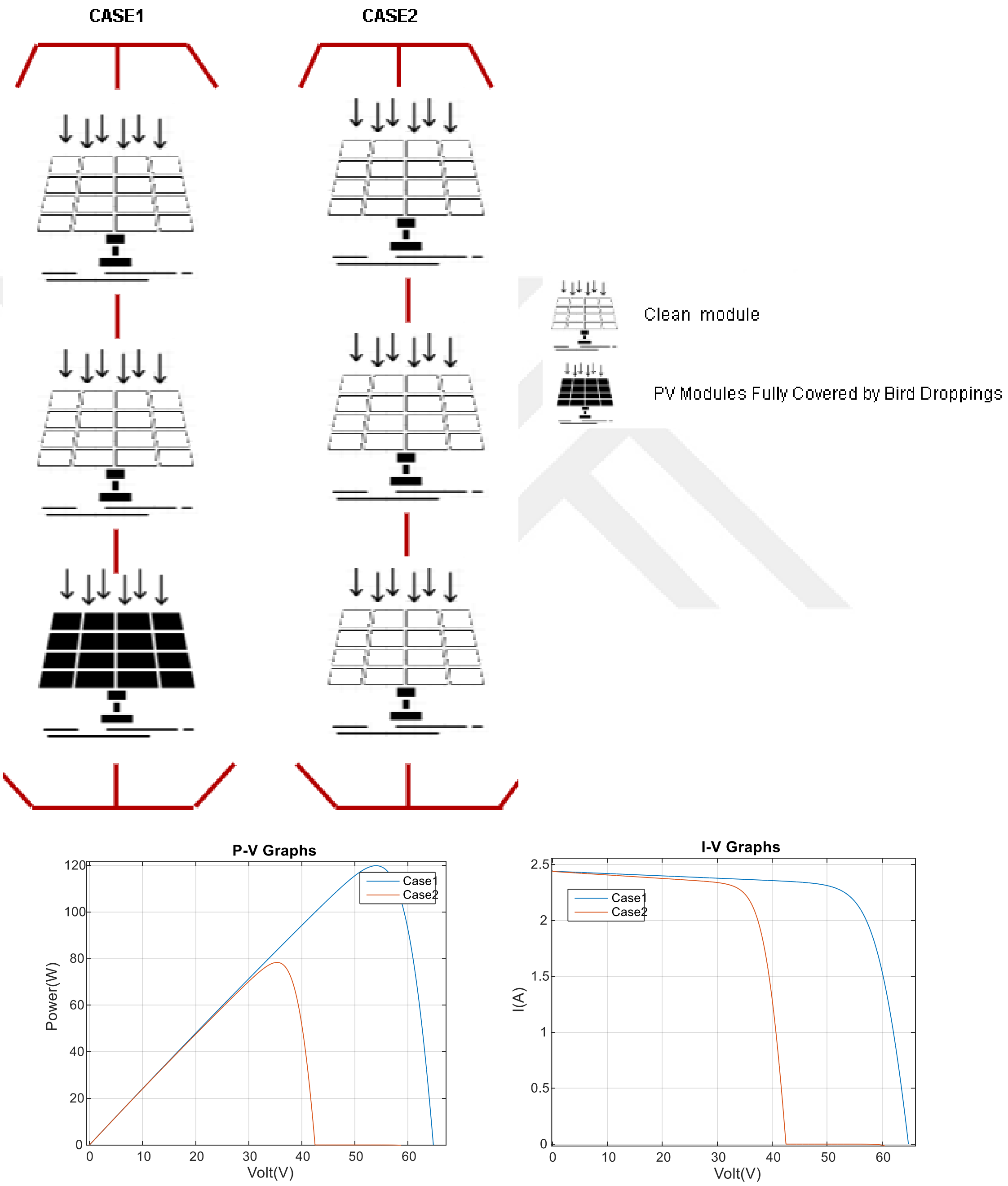

Figure 3.16. The PV modules fully covered by bird droppings.

3.3.7 Temperature impact on PV panel

High ambient temperature has an impact on the PV module performance, especially on the maximum power voltage. The higher cell temperature caused by higher ambient temperature results in a decrease in the maximum power voltage. It is shown in Figure 3.17.

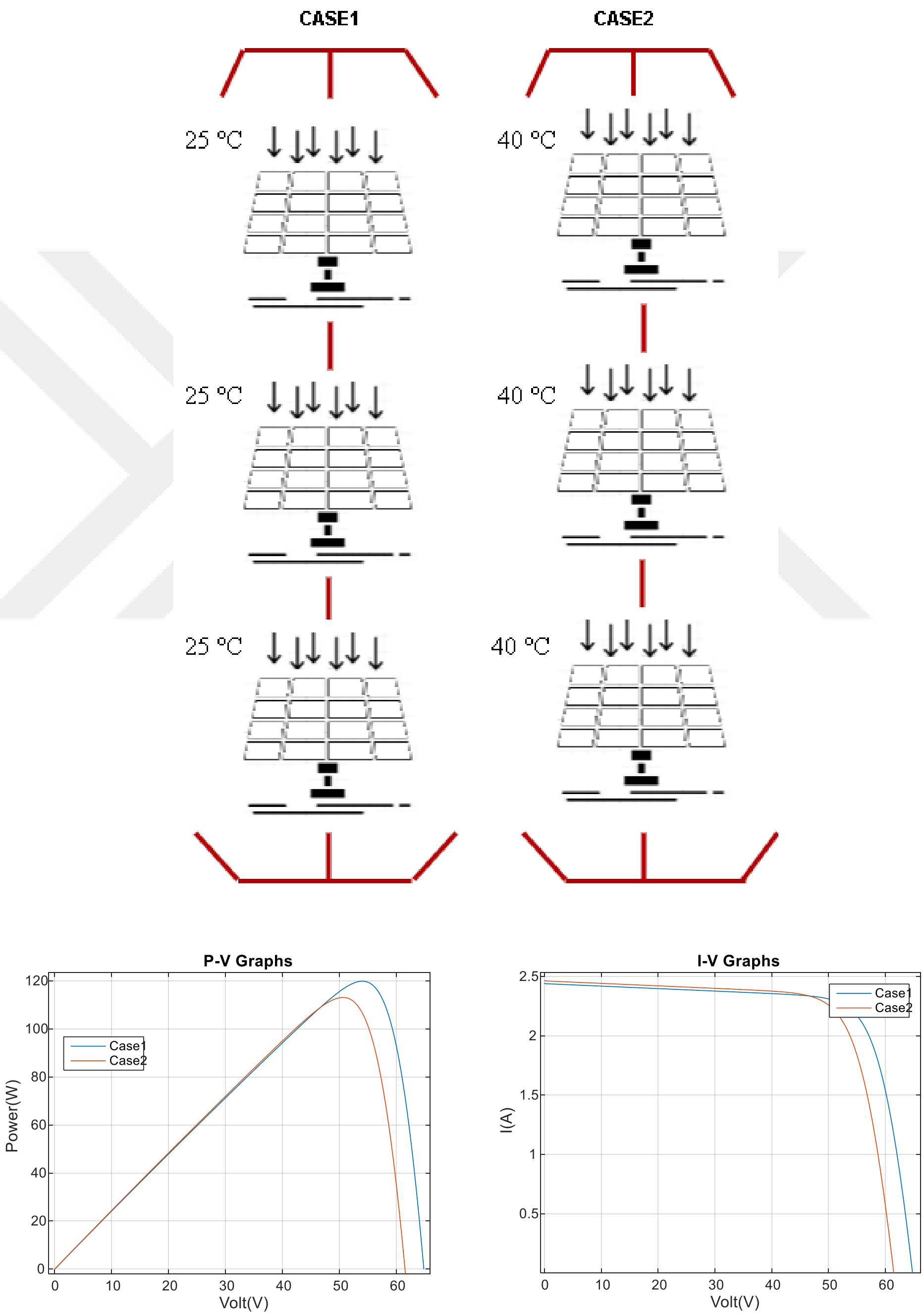

Figure 3.17. Temperature Impact on PV panel.

4. MATERIAL AND METHOD

Many changes in performance of the solar panels could not be seen. It needs to be inspected with more sophisticated tools [103]. For PV system fault detection, a small-scale lab test platform has been established. 40W PV modules are used for this purpose. This module is water-proof, lightweight, portable, and easily integrated for small appliances. It produces 18V under STC. There are 36 solar cells which are connected as series in the PV module. Each solar cell generates approximately 0.5V. There is a bypass diode located in the module's junction box. The PV module's electrical characteristics are given in Table 4.1. There are two main purposes of using this platform. One of them is used for thermal observation and the other one is used for UV observation.

Table 4. 1. The electrical characteristics of PV panel.

Open circuit voltage - Voc	24 V
Optimum operating voltage - Vmp	21 V
Short circuit current - Isc	1.7 A
Optimum operating current - Imp	1.3 A
Operating temperature	-40 to 85 C

4.1 Thermal/Infrared inspection

Any object above the absolute zero temperature (–273,15 °C = 0 Kelvin) emits electromagnetic radiation from its surfaces, and it is proportional to the internal temperature. Part of this inner radiation is infrared radiation, which can be used to measure the body temperature. Radiation emitted to the atmosphere is focused on the detector element with the help of a lens (input optics). Thus, a signal is generated depending on the radiation rate. The signals obtained can be used for process control on a screen or an analog output. There are obviously many advantages to using this system. Infrared system shown in Figure 4.1.

• Temperature measurements of moving or overheated objects and objects in hazardous surroundings

• Very fast response and exposure times

• Non interactive measurement, no influence on the measuring object

• Non-destructive measurement

• Measurement point durability, no mechanical wear

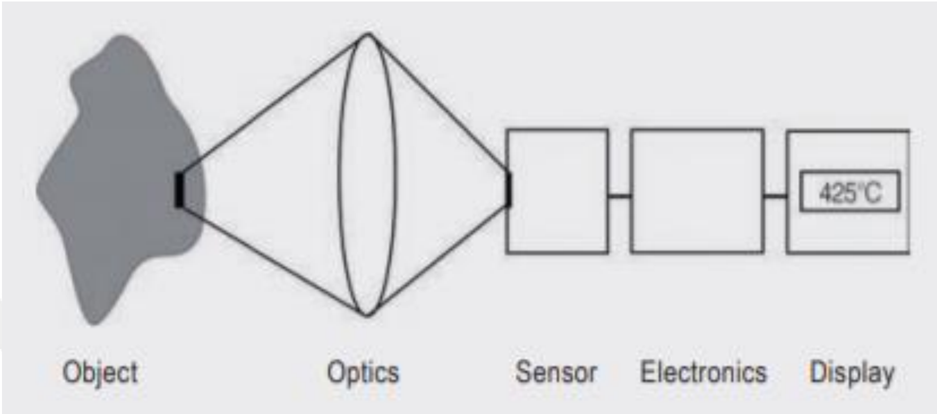

Figure 4.1. Infrared system.

To achieve thermal/infrared inspection, Optris Pİ160 brand thermal imager was used. The infrared camera has a measurement speed of 120 Hz and has 160 x 120 pixel optic resolutions. It is given in Figure 39. Technical specifications of Optris Pİ are given in Table 4.2.

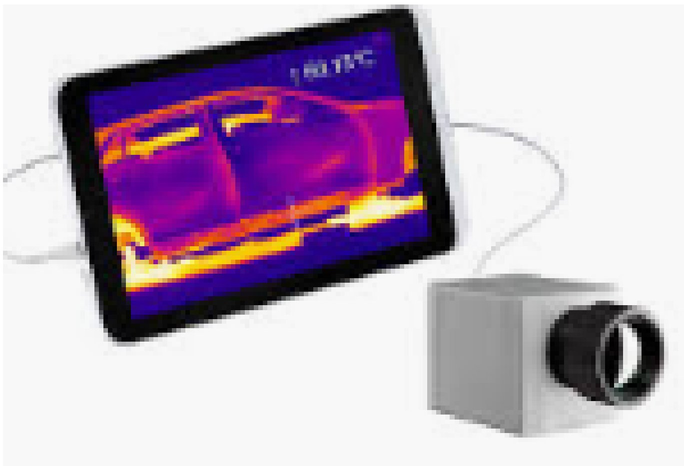

Figure 4.2. Optris Pİ160 thermal camera.

Table 4. 2 . Technical specifications of Optris Pİ 160 Thermal Camera.

1	***Frame rate***	*120 Hz.*
2	**Spectral range**	8 – 14 µm
3	**Temperature ranges**	–20 ... 100 °C, 0 ... 250 °C, (20) 150 ... 900 °C1), optional temperature range: 200 ... 1500 °C2)
4	**Optical resolution**	160 x 120 Pixel
5	**Accuracy**	±2 °C or ±2 %, whichever is greater
6	**Standard process interface**	0 – 10 V input, digital input (max. 24 V), 0 – 10 V output
7	**Power Supply:**	5 VDC (powered via USB 2.0 interface)
8	**Current draw:**	Max 500 mA

The distance of the object to be measured with thermal cameras is important. Different lenses can be used to take more precise measurements. Important parameters affecting the measurement are given in Figure4.3 which shows the connection between the distance of the measured object and the size of the pixel.

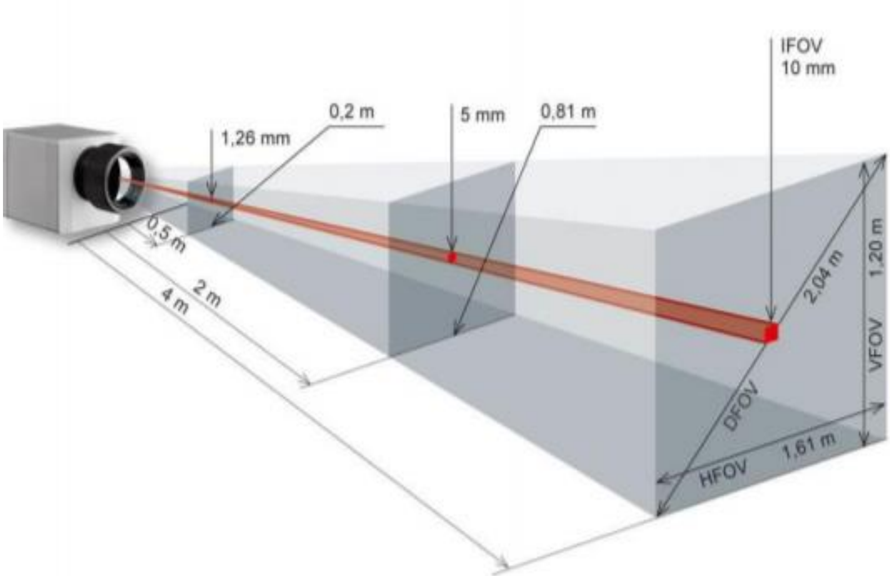

Figure 4.3. Measurement field of the infrared camera.

■ HFOV: Horizontal enlargement of the total measuring at object level

■ VFOV: Vertical enlargement of the total measuring at object level

■ IFOV: Size at the single pixel at object level

■ DFOV: Diagonal dimension of the total measuring field at object level

■ MFOV: Recommended, smallest measured object size of 3 x 3 pixel

There are two meters between the infrared camera and PV panel. The panel is set up about 90 degrees against the camera. Block diagram of test platform is shown in Figure 4.4.

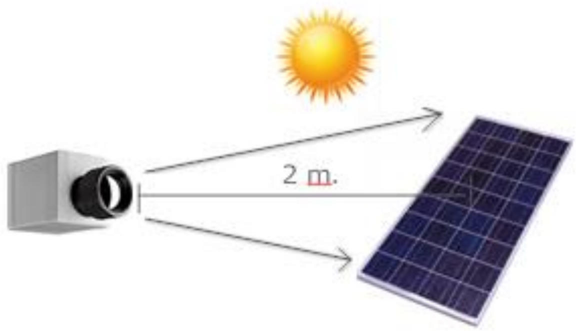

Figure 4.4. Block diagram of test platform.

4.1.1 Thermal/Infrared inspection methods

In this study, after the setting test platform, five different thermographic images were taken from the PV panel with a camera at regular intervals. It is given in Figure 4.5. They were used as reference images.

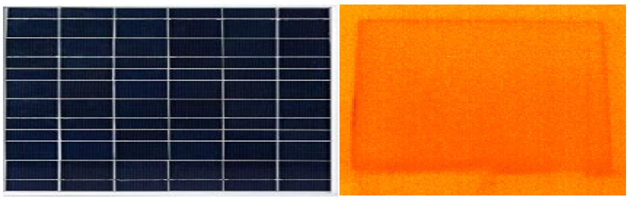

Figure 4.5. Polycrystaline panel and thermographic image.

Later, the PV panel parallel cells solders connection was broken. Then again, a thermographic image was captured from the panel. It is given in Figure 4.6. As a result of the broken parallel cells solders connections, the panel's power decreased from 40 W to 33 W. Also, the performance of the panel decreased to 17.5%.

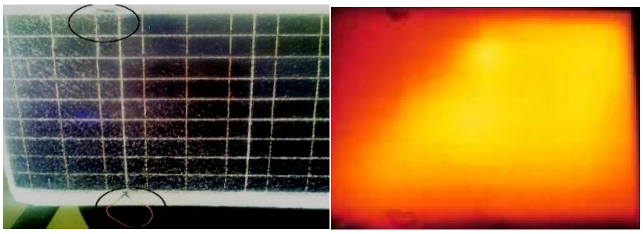

Figure 4.6. Fault polycrystaline panel and thermographic image.

The images were evaluated with Matlab. Thermographic image was read into the MATLAB using "imread" function. It is shown in Figure 43. Different areas were marked in each photo with MATLAB and RGB colour codes were obtained. To detect the broken cells effect on PV panel, sample images on the panel have been taken with periodic time intervals. Measurements regarding the PV panel are given in Table 4.3. In Table 4.3, a small voltage change can be seen in the fifth row with respect to the sixth row. The reason for this situation is broken solder connections. There is a linear increase between the PV panel output voltages.

Table 4.3. Measurement Data.

No	***Temperature(℃)***	***Output Voltage(V)***	***Time(s)***
1	28.1	9.47	12:17
2	28.7	10.04	12:31
3	29.2	10.16	12:46
4	29.8	10.24	13:02
5	30.3	10.58	13:18
6	29.9	10.9	14:03

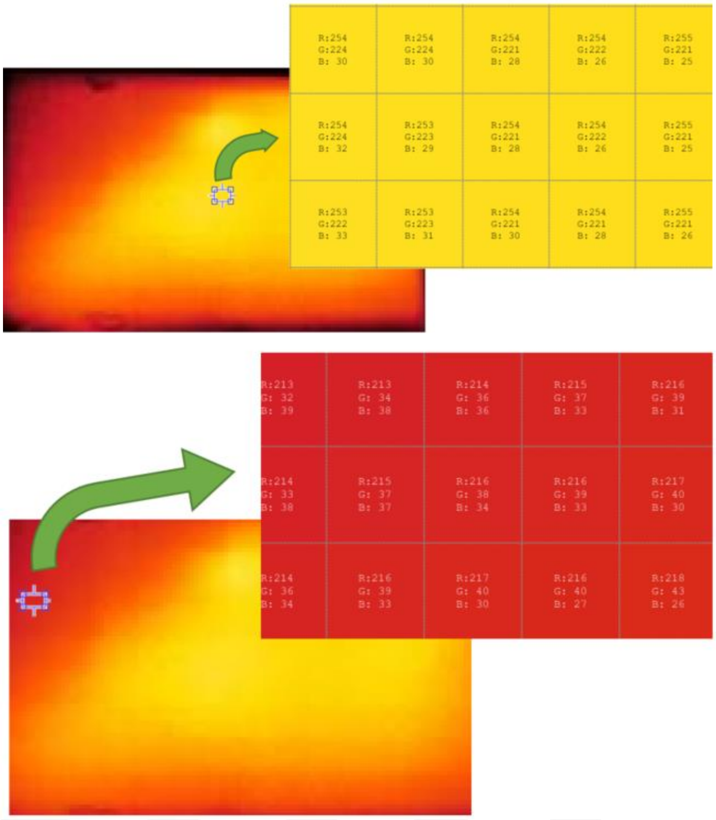

Figure 4.7. Average RGB values.

In general, there are almost 15 minute intervals for the panel output voltage measurements until the fifth row. But in the sixth row, the measurement has been made about 45 minutes later than other measurements. It is given in Figure 4.8. According to the linear interpolation calculations, the output voltage of the sixth row must be 11.4 V, but it was 10.9 V. The broken solder connection is the cause of this voltage drop.

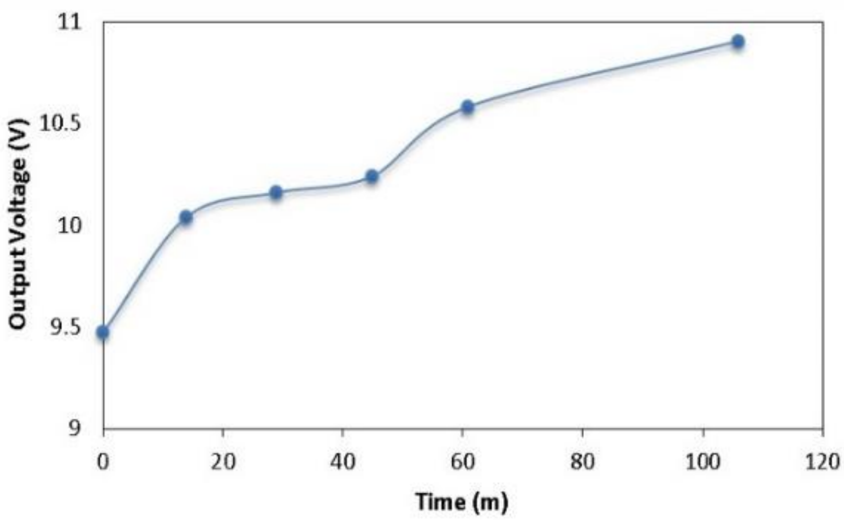

Figure 4.8. PV panel output voltage depends on the time.

It is clearly seen in this study that the situation of the panels can be observed with infrared cameras. Optris PI 160 brand thermal camera will be used between 800-1400nm spectral range. The reason for using the thermal camera is that the infrared wavelengths are too long for the human eye to detect and it is part of the electromagnetic spectrum that we perceive as heat. It also provides us a reference about whether the panel is faulty or not.

4.2 UV Inspection

In order to detect of PV module which has surface crack (due to snail train) and color changes, a rectangular shape detect box has been created. The system mainly consists of

1) six UV LED,
2) an Arduino electronics platform is used as controller,
3) an OPT101 photodiode,
4) a battery recharged,
5) a display,
6) a buzzer,
7) rectangular prism shape box, and
8) on-off switch.

A photodetector is an electronic device that converts incident photons into electric current. The texas instrument OPT101, block diagram and spectral responsivity are shown in Figure 4.9 The photodetectors are classified based on their optical range. The OPT101 is a photodiode which is a kind of on-chip trans impedance amplifier. This device is eliminates the problems such as electronics noise due to long wire leads, and makes fault detection device design easy [104]. The output voltage of the device increases linearly depending on the light intensity. Its operating voltage is between 2.7 V to 36 V, and quiescent current is only 120 μA. It has a light sensitive area of 2.286

x 2.286 mm. The photodetector has a responsivity of about 0.1 A/W (17 %) to the 400 nm light. The signal strength can increase if the photodetector has a maximum responsivity of 0.6 A/W (100 %) at 625 nm.

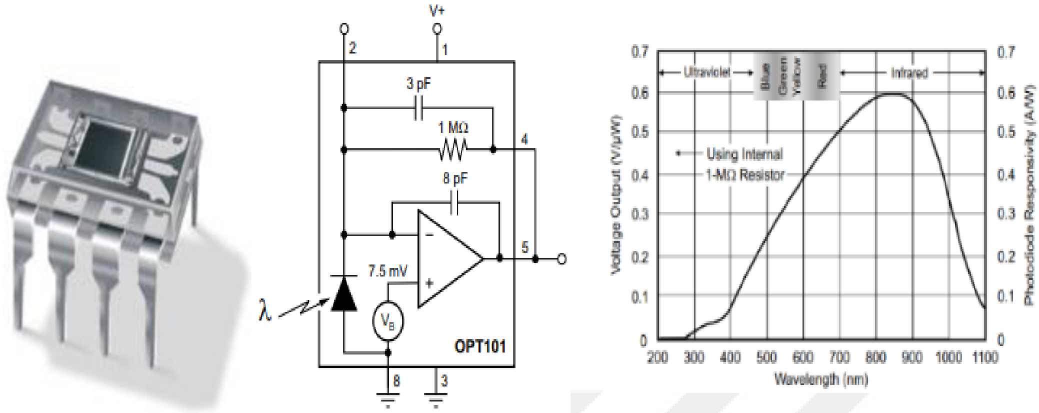

Figure 4.9. (a)Ti OPT101, (b) Block diagram, (c) Spectral responsivity.

Figure 4.10 describes the electrical architecture of the system and shows the spectral range of photodiode. The main controller has been realized by Arduino. OPT101 and UV LED are auxiliary for the system, but have as much importance as the controller. In addition, display and buzzer have been used as alert units in the system. OPT101 is a kind of detector and is widely used for testing physical materials. However, test materials could be biological, chemical liquids or any other type of material [105]. Its light sensitive area is between 2.286 x 2.286 mm [104]. The reflected light from the PV modules surface is transmitted. The UV LED spectrum is used within this range. The reason for choosing 390-410nm UV LEDs is being close to the electroluminescence (EL) spectrum and having cost efficiency. Also, the UV LED light is quite similar to the UV light in natural daylight [106].

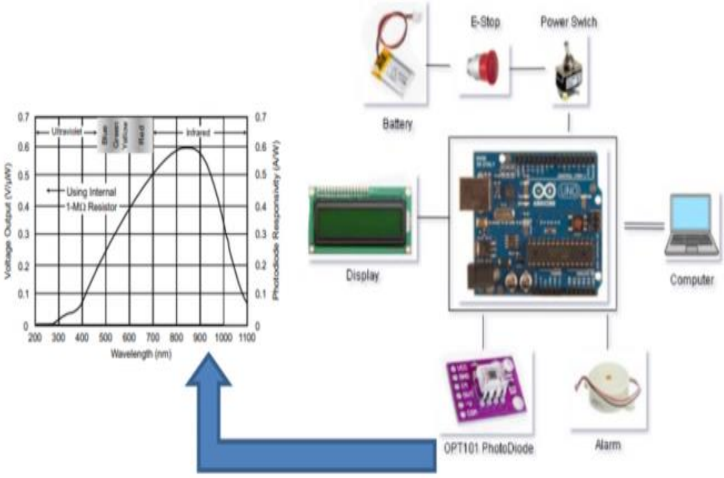

Figure 4.10. Electrical system architecture and spectral responsivity of OPT101.

Figure 4.11 shows a flow chart for detecting the degradation of the PV modules. The principle of operation is quite simple. The output voltage of the photodiode changes depending on the intensity of the light. Nominal operating value is determined before starting degradation detection. After, the degradation detection box starts to be moved as straight on the PV module. If the data obtained are very different from the nominal value, it can be said that there is a distortion within that area.

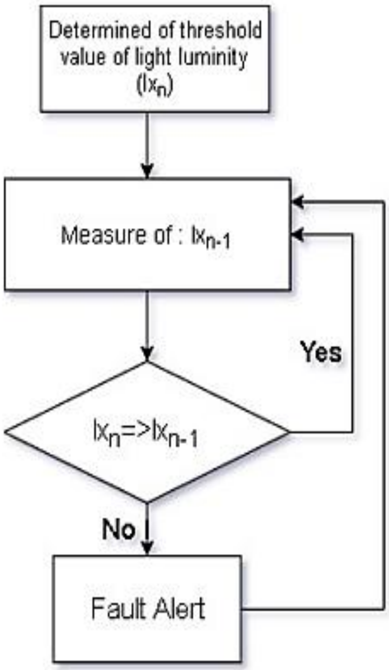

Figure 4.11. Algorithmic flow chart.

Depending on the wavelength range, the UV lights are divided into three groups: UV-A (longwave UV; 315-400 nm), UV-B (mediumwave UV; 280-315 nm), UV-C (shortwave UV;200-280 nm). In this study, 1W power UV led is chosen due to its cost, accessibility and applicability. Edixeon S series 1W power UV led shown in Figure 46. Its operating voltage is 3V and DC current is 350mA. Its wavelength is between 390-410 nm.

Figure 4.12. Edixeon S series 1W Power UV led.

4.2.1 UV inspection methods

Two experimental tests were carried out to detect the fault in PV panel in the laboratory:

- One of the tests was performed in the dark environment by applying UV led photon on the panel.
- In the other test, hot spot heating problem were detected by not using the UV LED.

The photons emitted from the UV led are reflected on the panel and then fall onto the photodiode shown in Figure 4.13.

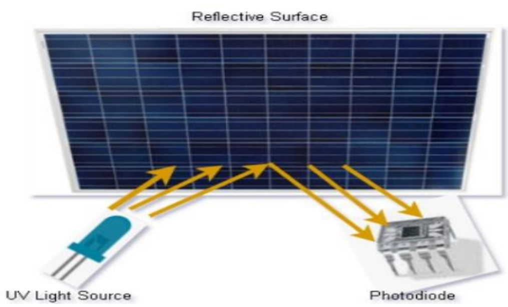

Figure 4.13. UV led and Photodiode testing equipment.

The led was located across the panel about 5 cm distance at an angle of 45 degrees. The photodiode was also located similarly. Both of them were placed in a rectangular prism shaped box shown in Figure 4.14.

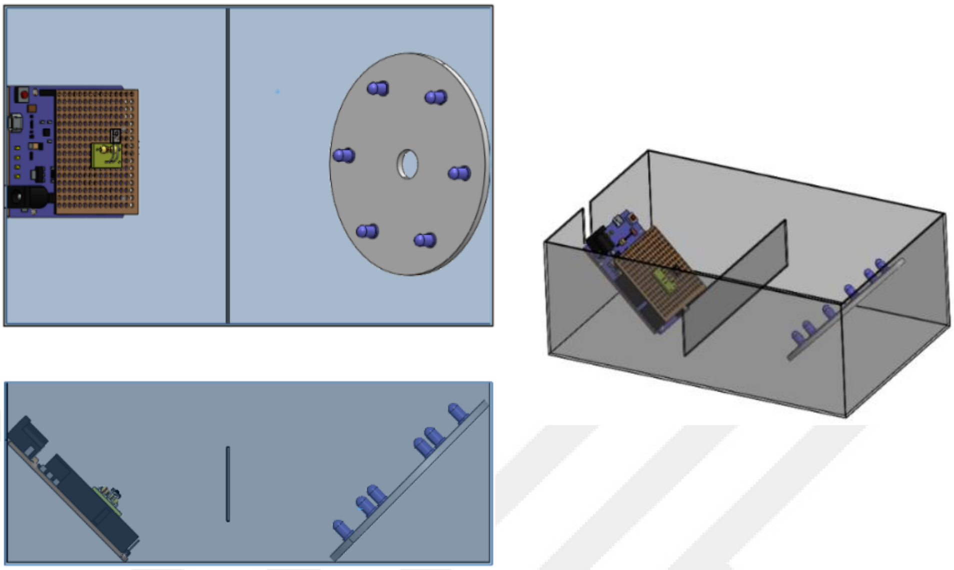

Figure 4.14. Photodetector test device solid design.

The output voltage of the photodiode changes depending on the intensity of the light falling on it. This voltage from the photodiode sensor are obtained by the Arduino uno programmable board with analog input pins. To do this, the pcb electronic card is designed (this enabled us to get rid of complicated cables and reduce electronic noise). With the "Serial.begin(9600)" and "Serial.println" functions, serial port is opened on the Arduino board and sensor data are sent to Matlab program (it is a multi-paradigm numerical computing software and a fourth generation programming language.). To do this, the correct COM Port must be selected and must be matched with both Arduino and Matlab Program. The Matlab GUI program was also created to display real-time data from the Arduino on a graph shown in Figure 4.15. There are some options in the MATLAB program like start, stop, and alert. Two seconds after the Start button is pressed, graphics start to be drawn. And when the stop button is pressed, the graphics drawing stops. The program was tested with collected data and obtained some graphical values.

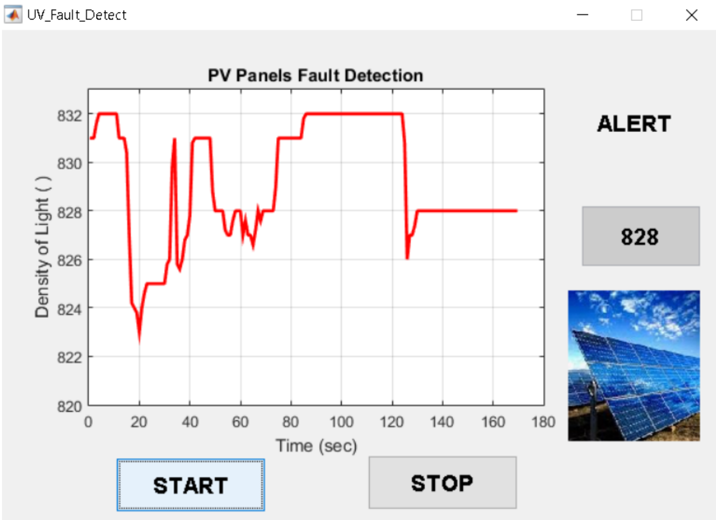

Figure 4.15. Matlab GUI program.

4.2.1.1 Yellowing fault inspection with UV led

The main objective of this study is to detect the degradation of the PV Modules. The results obtained from user interface software show that light reflected from colour changing cell area can be detected by the photodiode components easily. Figure 4.16 shows two different surfaces in the PV modules. While Figure 4.16 (A) has a homogeneous PV module appearance, Figure 4.16 (B) has nonhomogeneous colour appearance. The homogeneous and nonhomogeneous PV modules have been examined with this method and the results is shown in Figure4.17.

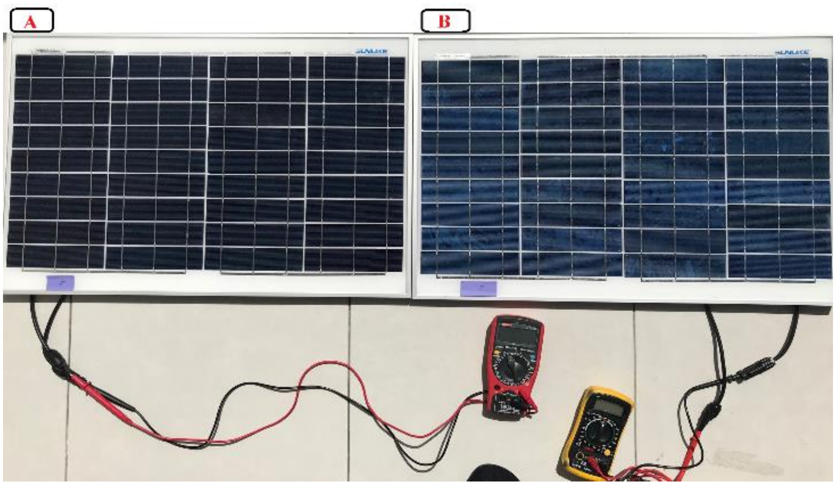

Figure 4.16. PV modules having two different surfaces.

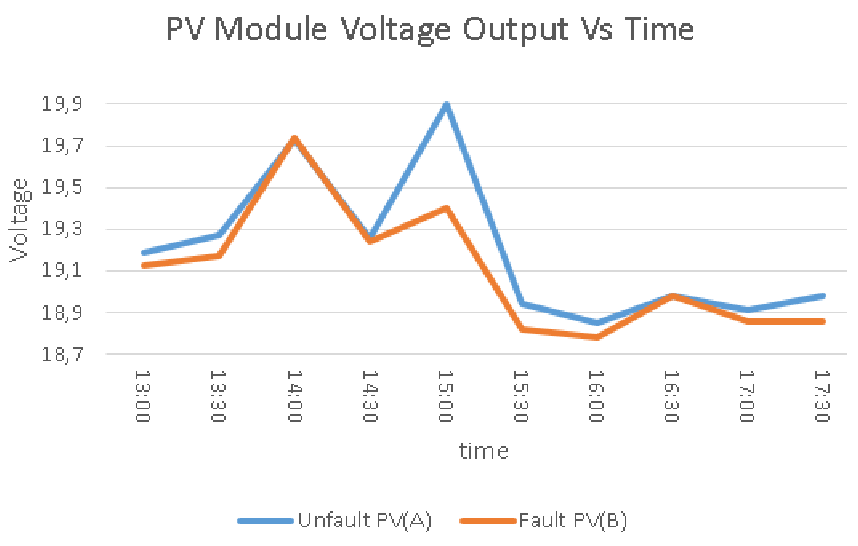

Figure 4.17. PV modules output voltages and time graphs.

Figure 4.18 show that there is an inverse proportion between the increase of surface temperature of modules and the output voltage. This situation is observed more clearly especially at 14:00 and 16:00 hours. The surface temperature has been obtained by Optris Pi160 thermal camera.

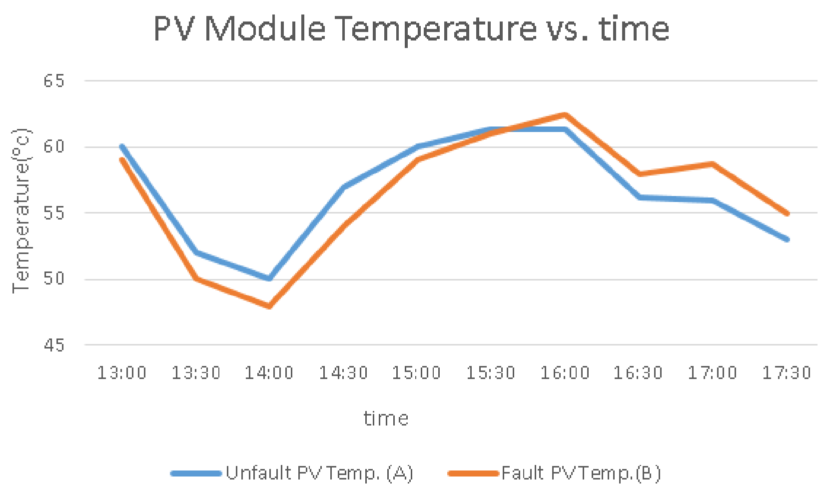

Figure 4.18. PV modules surfaces temperature and time graphs.

Figure 4.19 shows the thermal images of PV modules. It is a noncontact method to observe the module temperature and fault knowledge. However, this method may not always work to detect micro fractures on the panel. Figure 4.19 (A) shows the homogeneous module and Figure 4.19 (B) shows the nonhomogeneous module. The difference between the two modules cannot be obtained by thermal imaging.

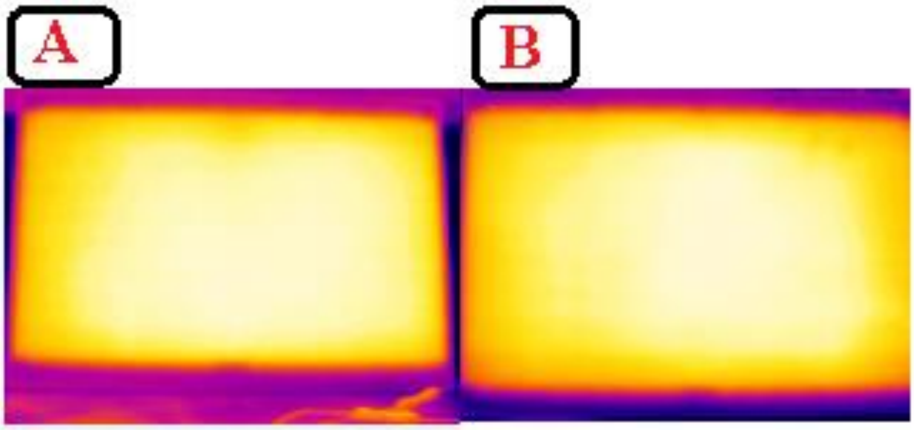

Figure 4.19. Thermal images of PV modules.

In addition, this study demonstrated that detecting the degradation in photovoltaic modules with UV led is easy and certain. Figure 4.20 shows a UV image of the PV module. The nonhomogeneous appearance has been clearly shown left side of Figure 4.20. Long term irradiation on the PV panel may lead to serious failures on its backsheet such as yellowing. The reason for the yellow colour is usually formation of chromophores [107]. When the PV panel that has yellowing part under the UV Led light is analysed, it is clear that these areas, which are sometimes difficult to see, have been noticed under UV led more easily. The colour changing parts were showen with numbers. Values that come from sensor on regions number 1, number 2 and number 3 plotted on the graphs in shown Figure 4.21.

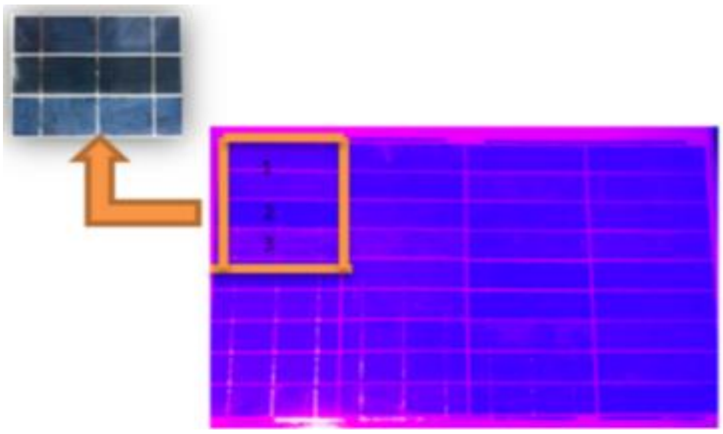

Figure 4.20. UV reflection image.

Figure 4.21 (a) and 4.21 (b) provide us the information about PV panel back sheet yellowing problem. Looking at the graph, an average value is seen as 826 on the nondefective cell on the PV panel under UV led. When the photodetector moved linearly from region #1 to region #3, changes on the values were observed. Nominal values are about 826, but yellowing region gives about 824-825. As a result, there is a difference between reflected light. The position, distance, resolution of the photodetector and scan time on the panel are the parameters that affect the system output. This method may be an inexpensive alternative to PV panel fault detection, but it requires time.

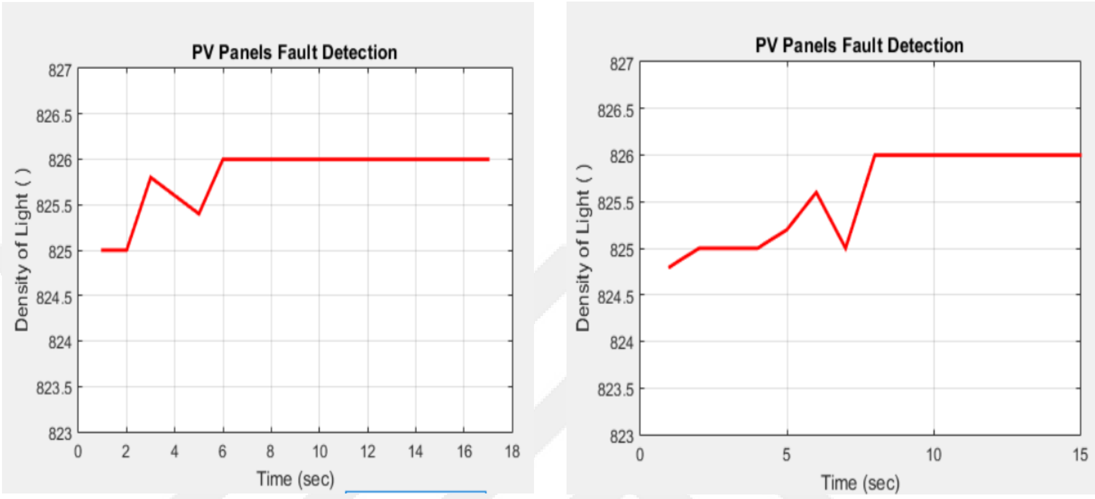

(a) (b)

Figure 4.21. UV led luminous intensity-time graphs.

4.2.1.2 Hot spot fault inspection without UV led

The shadow or dust layer falling on the panel reduces the current of the panel and reflects the light become in non-uniform form [108]. The change of irradiance is detected by the photodetector. It generates very small photocurrent values. To get high gain voltage and current, trans impedance amplifier is generally used. Performance of the amplifier affects the quality of this voltage signal. Choosing the appropriate amplifier is therefore important, that is why OPT 101 sensor was chosen in this study [104]. The system setup is shown in Figure 4.22. In this experimental study, a white light bulb was used to simulate daylight. An object was placed on the panel to make a shadow. When the photodetector is on the shaded surface, changes on the data are observed and shown in Figure 4.23.

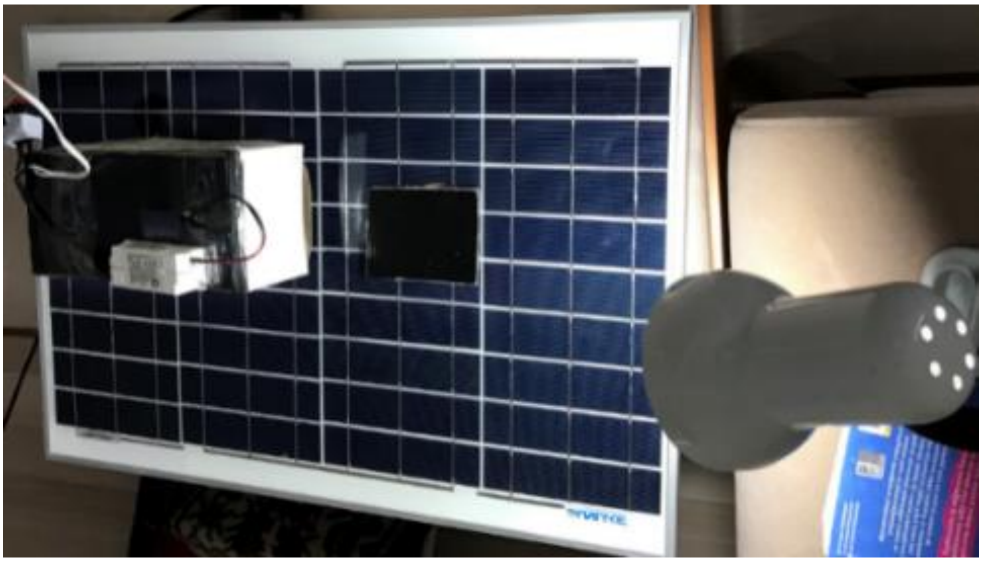

Figure 4.22. Photodetector test device without UV LED.

Figure 4.23 (a), (b), (c) and (d) graphs provide us the information about reflected beam. In Figure 4.23, the graphs in (a), (b) and (c) show that the detector passes once over the shaded surface. And the graphs in (d) shows that the detector passes two times over the shaded surface. The photodetector produces an average value without UV led about 831-832. When the photodetector came on the shaded surface, the average value of the sensor decreases.

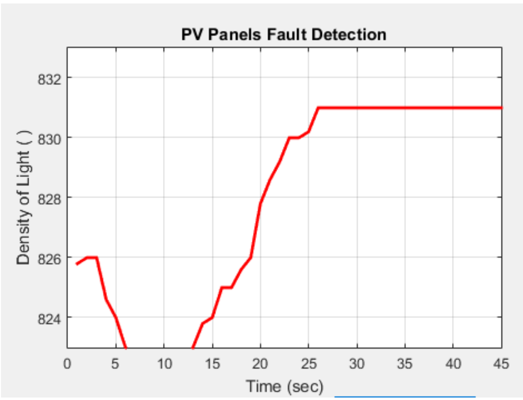

(a)

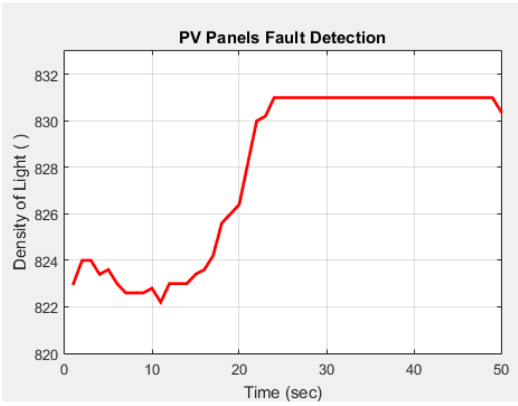

(b)

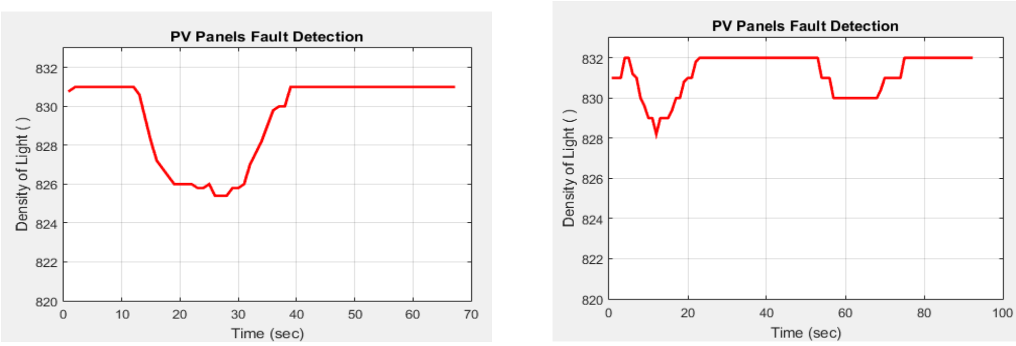

(c) (d)

Figure 4.23. Luminous intensity-time graphs without UV LED.

4.2.2. Colour change detection on PV panel in visible spectrum

It has seven wavelength ranges which are coordinated to different colours. When the move from red to violet, energies of spectrum have been increased and the wavelength of spectrum have been decreased. Different types of wavelengths are given below.

- Violet - 400-420 nm
- Indigo - 420 - 440 nm
- Blue - 440 - 490 nm
- Green - 490 - 570 nm
- Yellow - 570 - 585 nm
- Orange - 585 - 620 nm
- Red - longest wavelength, at around 620 - 780 nanometres with lowest frequency

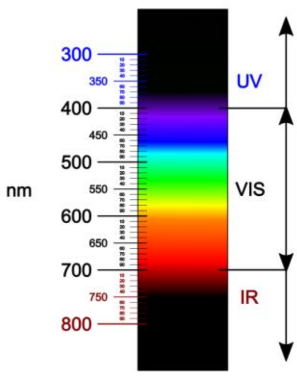

Figure 4.24. Visible spectrum [79].

To obtain the colour changes on the PV panel in the visible spectrum, the experimental setup has been prepared. Step Motor, step motor driver, one-meter ball screw, microcontroller and power supply have been used. In table 4.4 step motor electrical characteristics has been given. Figure 4.25 shows all mechanical systems. The speed of the screw was adjusted software-wise, approximately 5 mm per second. The distance of the photodiode sensor from the surface is about 3 cm. The results were examined in four different visible lights which are Blue, Red, Green, and Yellow in the visible spectrum.

Table 4.4. Step Motor electrical specifications

Voltage	5.9V
Current	4.2A
Inductance	9Mh
Resistance	1.4ohm
Holding Torque	110Kg.cm
Step Angle	1.8

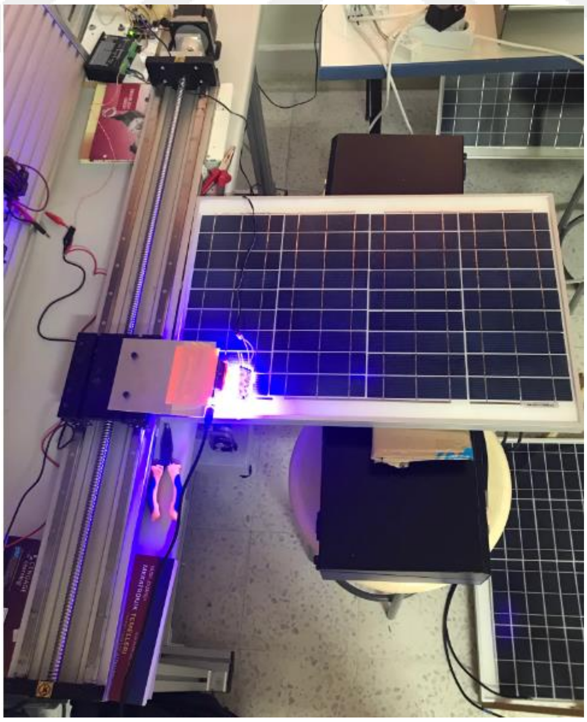

Figure 4.25. Luminous intensity-time graphs without UV LED.

4.2.2.1. Blue led inspection

The blue light is close to the UV spectrum area and it has 440 - 490 nm wavelength. Color changes on the panel are observed from the graphic. The intervals between 50-100 seconds on the graph and about 280-330 seconds are the regions where the color changes on the panel. Blue light is the wavelength at which the change is most clearly achieved in the visible spectrum.

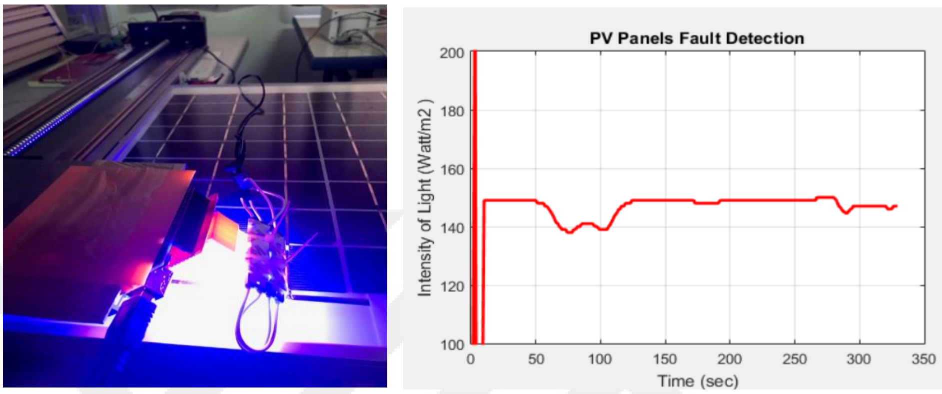

Figure 4.26. Blue LED inspection.

4.2.2.2. Red led inspection

It has longest wavelength, at around 620 - 780 nanometres with lowest frequency. In addition, brightness of about 140 was obtained from reflections. Color changes on the PV panel are not clearly achieved.

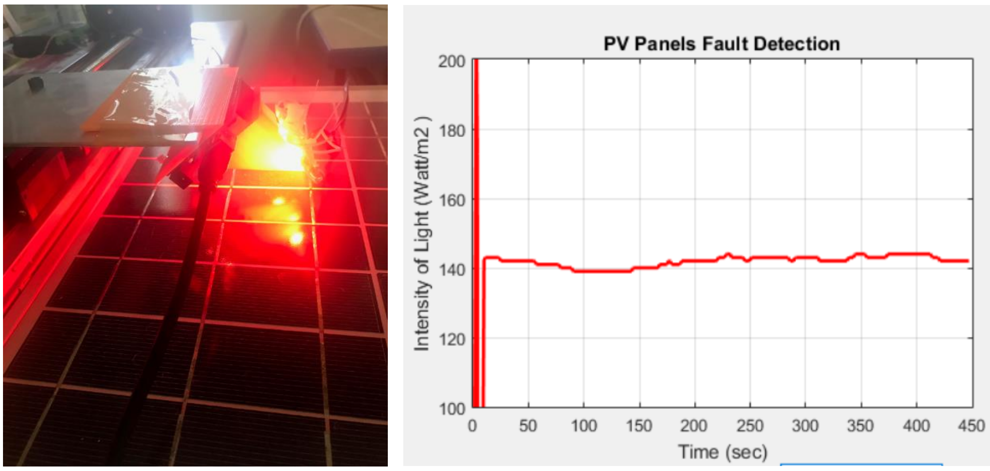

Figure 4.27. Red LED inspection.

4.2.2.3. Green led inspection

It has 490 - 570 nm spectrum wavelength. The brightness value reflected from the PV panel is about 160. Colour change on the panel cannot be achieved in this spectrum.

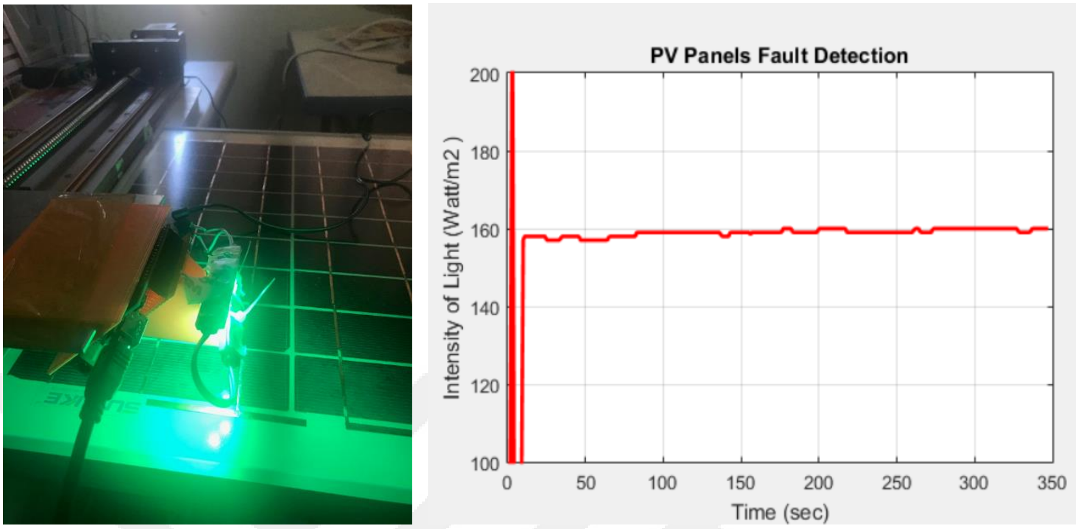

Figure 4.28. Green LED inspection.

4.2.2.4. Yellow led inspection

It has 570 - 585 nm spectrum wavelength. The brightness value reflected from the PV panel is about 147. Colour change on the panel cannot be achieved in this spectrum.

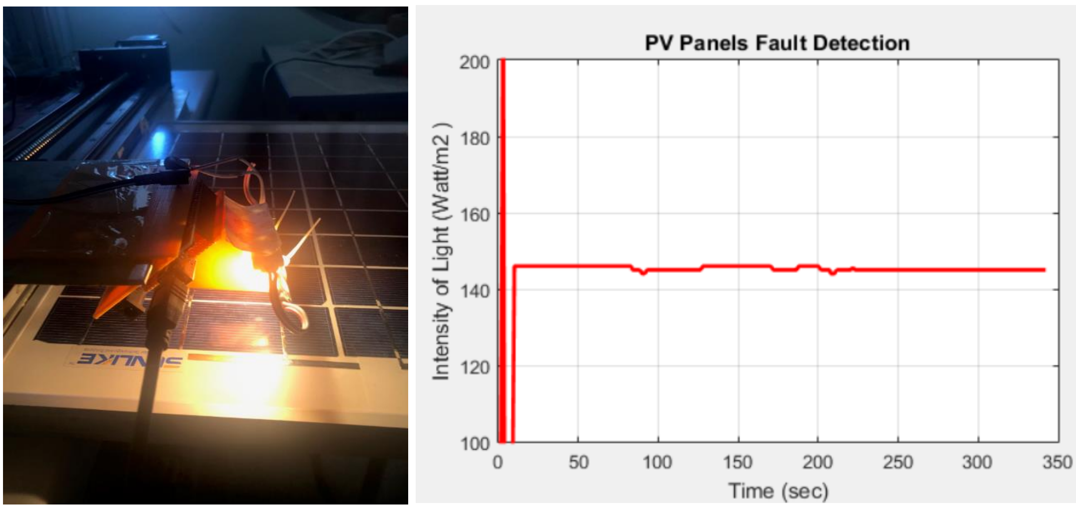

Figure 4.29. Yellow LED inspection.

4.3 Other Inspection Method

4.3.1 Electroluminescence

Electroluminescent (EL) is a very useful diagnosis tool for fault detection. With this method used in the cells and modules defects like cracks (ELCD; Electroluminescence Crack Detection Test), technological defects and other inhomogeneities faults are diagnosed. Therefore, it is a kind of diagnostic tool that can also be used for the visual inspection of modules. Electroluminescence is an optical as the electrical phenomenon where the material releases light when either electric current flows in it or a strong electric field is applied across it. It works at the principle of optics [109].

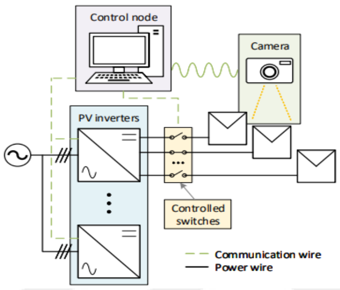

Figure 4.30. EL maintenance technique [110].

Generally, three types of sensors are used in the EL system such as cooled CCD (Charge-Coupled Device), CMOS and InGaAs. The sensor must be placed in a sufficiently dark area to detect the faulty area on the panel.

4.3.2 Photoluminescence

Photoluminescence is a process which is used for PV cells diagnostics[109]. There are two type of this method such as fluorescence and phosphorescence. It is used to detect faults of the panel during the production process by the strong light impulse with the excited-state method without touching the panel. It is used to detect faults of the panel during the production process by the strong light impulse with the excited-state method without touching the panel.

4.3.3 Microplasma Luminescence

This method gives information about the fractures on the PV panel[109].

5. CONCLUSION

Solar energy works on a simple principle which is that the sunshine falls on solar cell which converts sunlight into electricity. When sunlight hits the surface of a panel, it excites electrons in the cells, and they start to flow out as direct current. The direct current gets converted to alternating current using inverters and finally in most cases this clean and renewable form of energy gets exported to the grid on a large scale. This system requires a large area to generate electricity. Today, their productivity is still not at the desired level. It requires about a land of 20 acres per MW. Therefore, dozens of megawatts of electricity are required for large areas. This situation leads to a difficulty in maintenance. There are many studies in the literature about the fault detection of PV panels. Rather than fault detecting, it is important to maintain the possible states of the panels before they become faults and to protect the PV panel.

In this thesis study, the most common types of faults were discussed and simulation studies were carried out. It is illustrated in APPENDIX A-1: Simulation Result of PV Panel with Fault Scenario Scenarios that containing fault types were created. Shading case, line to line fault, soiling problem that the annual losses caused by soiling between 3-6 % and 14% [111], degradation: increase in resistance between module cell problem, bird droppings-tree leaves problem, and temperature impacts on PV module. All these scenarios are encountered in PV systems.

Also, in the laboratory environment, the cells which the series connected on the PV panel were disconnected and it was observed whether they could be detected in the infrared spectrum. As a result of this experimental study, a temperature increase on the panel was observed after disconnected cells. It is shown in APPENDIX A-2; c and d parts clearly.

In addition, another experimental study was carried out in the UV spectrum level, so that the yellowing PV panel cells can be detected. Yellowing is one of the serious problems that may occur in PV panels that are exposed to radiation for a long time. It is formed by the formation of chromophores, which are portions of macromolecular chains that selectively absorb the different frequencies of visible light, giving colour to molecules [107]. It is shown in APPENDIX A-2; a and b parts clearly. In the interface developed with Matlab/Simulink program, it is observed that the signal output data of the yellowing region is different.

Besides, colour changes on the PV panel were tried to be determined at different spectrum values. Blue, green, yellow and red LED have been used for this purpose. It is understood from the figure that the blue led spectrum is most effective method to obtain PV diagnosis. According to the results obtained, it was observed that colour changes on the PV panel could not be obtained in colours other than blue.

Also, hot spot heating problem caused by shading falling on the panel was investigated. To do this, an object is located on different surfaces of the panel. It was observed that when compared to the signal output caused by the object placed on the surface was different from the unshaded part of the PV module. The output signal is received via the Arduino control card and transmitted in series to the MATLAB program.

5.1 Future Work

Electricity consumption is expected to reach 375.8 TWh in 2023 [112]. Total electricity generation in 2018 is 303625 GWh. Resource distributions is shown in Figure 5.1. In the last three years (2016-2018), electricity generation from PV panels has increased from 1043GWh to 7477GWh [113].

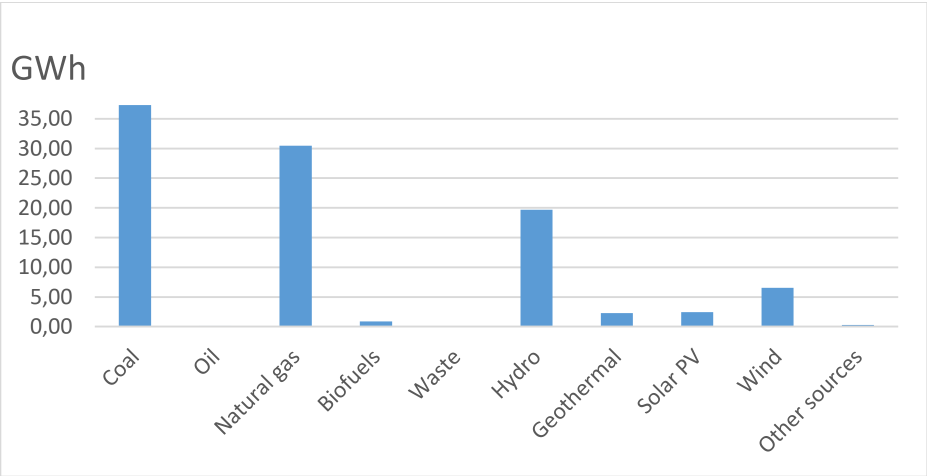

Figure 5.1. Turkey electricity generation resources-2018.

The percentage of electricity generated from PV panels in total sources increased from 0.38 to 2.46. The rate of electricity produced from PVs increases approximately twice per year. It is clear that this situation shows the importance of PV panels among energy sources. In addition, fault in photovoltaic panels affects the amount of electricity generated. Maintenance and fault detection speed is very important in order not to reduce the amount of electricity generated. One of the fault detection methods suggested in the thesis is the UV led error detection is very important in this regard. In the future studies, this method may be used on an autonomous robotic system. The robot system may be designed as to move on the PV panel. In addition, pollution and dust on the panel can be prevented by the cleaning apparatus to be placed on the robot. In the literature, energy losses due to pollution vary between 3% and 14%. This is a fairly high rate.

In addition, the types of faults in different spectrum ranges can be examined as future studies. Thus, the cheaper fault detection method could be investigated.

REFERENCES

1. Çanka, F., 2015. Solar energy, its recent status in turkey and production technologies güneş enerjisi, türkiye'deki son durumu ve üretim teknolojileri, Mühendis ve Makina, 56, 671, 28–40.

2. URL-1 < https://www.iea.org/reports/renewables-2019 >, Date of access:20.05.2020.

3. Tabak, A., 2019. Grey wolf optimization for optimum sizing and controlling of a pv/wt/bm hybrid energy system considering tnpc, lpsp, and lcoe concepts, Energy Sources, Part A Recovery, Utilization and Environmental Effects, 1, 3, 1-21.

4. URL-2 < https://www.irena.org > , Date of access: 21.05.2020.

5. URL-3 < https://www.infiniteenergy.com.au/module-efficiency-mean > , Date of access: 21.05.2020.

6. Solanki, P.C., 2008. Solar photovoltaic technologies, The Sun and PV technologies. First Edition, Springer, Switzerland.

7. Hammoud, M., 2019. Effect of dust cleaning on the enhancement of the power generation of a coastal PV-power plant at Zahrani Lebanon, Solar Energy, 184, 1, 195–201.

8. Čorba, Z.J., 2012. In-Grid solar-to-electrical energy conversion system modeling and testing, Thermal Science, 16, 1, 159-171.

9. Jazayeri, K., 2012. Determination of power losses in solar panels using artificial neural network, Ph. D. thesis, Eastern Mediterranean University, Northern Cyprus.

10. Moon, E., 2017. Subcutaneous photovoltaic infrared energy harvesting for bio-implantable devices, IEEE Transactions on Electron Devices, 64, 5, 2432-2437.

11. Gan, P. Y., 2015. Quantitative study on long term global solar photovoltaic market, Renewable and Sustainable Energy Reviews, 46, 1, 88–99.

12. Sharma, V., 2013. Performance and degradation analysis for long term reliability of solar photovoltaic systems : A review, Renewable and Sustainable Energy Reviews, 27,1, 753–767.

13. Tsanakas, J. A., 2017. Advanced inspection of photovoltaic installations by aerial triangulation and terrestrial georeferencing of thermal / visual imagery, Renewable Energy, 102, 1, 224–233.

14. Omazic, A. 2019. Relation between degradation of polymeric components in crystalline silicon PV module and climatic conditions: a literature review, Solar Energy Materials and Solar Cells, 192,4, 123–133.

15. Chaichan, M. T. and Kazem H.A., 2018. Environmental Conditions and Its Effect on PV Performance, First Edition, Springer.

16. Guiheneuf, V., 2017. Effects of the irradiance intensity during UV accelerated aging test on unencapsulated silicon solar cells, Solar Energy, 157, 4, 477–485.

17. Kaplani, E., 2016. Renewable energy in the service of mankind, Renewable Energy Services, 4, 2, 393-402.

18. Sinha, A., 2016. Nondestructive characterization of encapsulant discoloration effects in crystalline-silicon PV modules, Solar Energy Materials and Solar Cells, 155, 1, 234–242.

19. Gagliardi, M., 2017. Solar energy materials and solar cells a reaction-di ff usion formulation to simulate eva polymer degradation in environmental and accelerated ageing conditions, Solar Energy Materials and Solar Cells, 164, 2, 10, 93–106.

20. Liu, Z., 2019. Quantitative analysis of degradation mechanisms in 30-year-old pv modules, Solar Energy Materials and Solar Cells, 200, 6, 110-119.

21. Peike, C., 2011. Non-destructive degradation analysis of encapsulants in pv modules by raman spectroscopy, Solar Energy Materials and Solar Cells, 95 , 7, 1686-1693.

22. Meyer, E. L., 2004. Assessing the reliability and degradation of photovoltaic module performance parameters, IEEE Transactions on Reliability, 53, 1, 83-92.

23. Kim, T. H., 2013. The effect of moisture on the degradation mechanism of multi-crystalline silicon photovoltaic module, Microelectronic Reliabillity, 53, 9, 1823–1827.

24. Sibiński, M. , 2017. Degradation of flexible thin-film solar cells due to a mechanical strain, Opto electronics Review, 25, 1, 33–36.

25. Kichou, S., 2017. Automatic supervision of PV systems and degradation analysis of thin film PV modules, Ph. D. thesis, University Politècnica de Catalunya, Barselona.

26. Liu, F., 2014. Ultra-Violet degradation behavior of polymeric backsheets for photovoltaic modules, Solar Energy, 108, 4, 88-100.

27. Kobi, A., 2013. Degradations of silicon photovoltaic modules : A literature review, Solar Energy 96, 2, 140-151.

28. Patel, J.B., 2019. Effect of ultraviolet radiation on organic photovoltaic materials and devices, ACS Applied Materials and Interfaces, 11, 24, 21543-21551.

29. Dolara, A., 2014. Investigation on performance decay on photovoltaic modules: snail trails and cell microcracks, Photovoltaics, 4 5, 1204-1211.

30. Meyer, S., 2013, Snail Trails : root cause analysis and test procedures, Energy Procedia, 38, 4, 498-505.

31. Dolara, A., 2016. Snail trails and cell microcrack impact on pv module maximum power and energy production, IEEE Journal of Photovoltaics, 6 , 5, 1269-1277.

32. Boppana, S., Rajasekar, V. and Tamizhmani, G., 2015. Working towards the development of a standardized artificial soiling method, IEEE 42nd Photovoltaic Specialists. Conference PVSC 2015, pp. 1–6, 2015.

33. Liu, F. Jiang, L. and Yang, S., 2014. Ultra-violet degradation behavior of polymeric backsheets for photovoltaic modules, Solar Energy, 108, 10, 88–100.

34. Wu, X., 2011. Fault detection and diagnosis of photovoltaic systems, Master Thesis, University Of Southern California, USA.

35. Yerebakan, M., 2010. Güneş enerjisi kullaniminin tarihsel gelişimi ve türkiye’deki yeri, Hyperlinks, 1, 1, 36-38.

36. Jazayeri, K., 2012. Determination of Power Losses in Solar Panels Using Artificial Neural Network, Master thesis, Eastern Mediterranean University, Electrical and Electronic Engineering, Gazimağusa, North Cyprus.

37. URL-4 < https://www.iea.org/reports/technology-roadmap-solar-photovoltaic-energy-2010> , Date of access:01.02.2020.

38. Mahto, R. V., Sharma, D. K., Xavier, D. X. and Raghavan, R. N., 2020. Improving performance of photovoltaic panel by reconfigurability in partial shading condition, Journal of Photonics Energy, 10, 4, 042004.

39. Adıgüzel, E., Özer, E., Akgündoğdu, A. and Ersoy Yılmaz, A., 2019. Prediction of dust particle size effect on efficiency of photovoltaic modules with ANFIS: An experimental study in Aegean region, Turkey, Solar Energy, 177,1, 690–702.

40. Yamaguchi M., Lee, K. H., Araki, K., Kojima, N. and Ohshita, Y., 2018. Analysis for efficiency potential of crystalline Si solar cells, Journal of Materials Research, 33, 17, 2621–2626.

41. Zulkefli, M.Z., Rusli, N., Hashim, N.A., Jamian, J.J. and Abdullah, M.N., 2017 Investigation of solar photovoltaic performance via cooling-light concentrating and cleaning system using robotic arduino approach, Proc. 2017 6th International Conference Electronics Engineering and Informatics ICEEI 1, 1–6.

42. Akyazı, Ö., Şahin, E., Özsoy, T. and Algül, M., 2019. A solar panel cleaning robot design and application, European. Journal of Science and Technology, 1, 1, 343–348.

43. Chaichan, M.T., Kazem, H.A., Chaichan, M.T. and Kazem, H.A., 2018. Environmental Conditions and Its Effect on PV Performance, First Edition, Springer International Publishing, 82-129.

44. Patel J.B., 2019. Effect of Ultraviolet Radiation on Organic Photovoltaic Materials and Devices, ACS Appl. Mater. Interfaces, 11, 24, 21543–21551.

45. Irwanto, M., Irwan, Y.M., Safwati, I., Leow W.Z. and Gomesh, N. 2014. Analysis simulation of the photovoltaic output performance, IEEE 8th International Power Engineering and Optimization Conference, 1, 4, 477–481.

46. Adinoyi, M. J. and Said, S.A.M., 2013. Effect of dust accumulation on the power outputs of solar photovoltaic modules, Renewable Energy, 60, 6, 633–636.

47. Mani M. and Pillai, R., 2010. Impact of dust on solar photovoltaic (PV) performance: Research status, challenges and recommendations, Renewable and Sustainable Energy Reviews, 14, 9, 3124–3131.

48. Abass, K.I., Al-zubaidi S. M. and Al-waeli, A. A. K., 2017. Effect of pollution and dust on PV performance, International Journal of Civil, Mechanical and Energy Science (IJCMES) 3, 4, 181-185.

49. Guo, B., Javed, W., Figgis, B. and Mirza, T., 2015. Effect of dust and weather conditions on photovoltaic performance in Doha , Conference: Smart Grid and renewable Energy (SGRE), Qatar, 01,02,10-15.

50. Salimi, H., Mirabdolah Lavasani, A., Ahmadi-Danesh-Ashtiani, H. and Fazaeli, R., 2019. Effect of dust concentration, wind speed, and relative humidity on the performance of photovoltaic panels in Tehran, Energy Sources, Part A Recover. Util. Environ. Eff., 00, 00, 1–11.

51. Chaichan, M. T. and Kazem, H. A. 2020. Experimental evaluation of dust composition impact on photovoltaic performance in Iraq, Energy Sources, Part A Recovery, Utilization and Environmental Effects, 00, 00, 1–22.

52. Kazem, H. A. and Chaichan, M. T. 2019. The effect of dust accumulation and cleaning methods on PV panels' outcomes based on an experimental study of six locations in Northern Oman, Solar Energy, 187, 5, 30–38.

53. Lu, H. and Zhao, W., 2019. CFD prediction of dust pollution and impact on an isolated ground-mounted solar photovoltaic system, Renewable Energy, 131, 1, 829–840.

54. Chakkarapani, R.M., Saravana Ilango, G. and Nagamani, C., 2016. A method to detect photovoltaic array faults and partial shading in pv systems, IEEE Journal of Photovoltaics, 6, 5, 1278–1285.

55. Jenitha, P. and Immanuel Selvakumar, A., Fault detection in PV systems, Applied Solar Energy, 12, 03,10-18.

56. Platon, R., Martel, J., Woodruff, N. and Chau, T., Y. 2015. Online fault detection

in pv systems, IEEE Transactions Sustainable Energy, 4,10, 10-17.

57. Alsafasfeh, M., Abdel-Qader, I., Bazuin, B., Alsafasfeh, Q. and Su, W., 2018. Unsupervised fault detection and analysis for large photovoltaic systems using drones and machine vision, Energies, 11, 1, 20-26.

58. Tadj, M., Benmouiza, K., Cheknane, A. and Silvestre, S., 2014. Improving the performance of PV systems by faults detection using GISTEL approach," Energy Conversion Management, 80, 03, 298–304.

59. Garoudja, E., Harrou, F., Sun, Y., Kara, K., Chouder, A. and Silvestre, S., 2017. Statistical fault detection in photovoltaic systems, Solar Energy, 150, 3, 485–499.

60. Özkişi, H. and Topaloğlu, M., 2017. Fotovoltaik hücrenin verimliliğinin yapay sinir ağı ile tahmini, Bilişim Teknoloji. Dergisi, 10, 3, 247–253.

61. Karafil, A., Ozbay, H. and Kesler, M., 2016. Temperature and solar radiation effects on photovoltaic panel power, Journal of New Result Science, 12, 48–58.

62. Salmi, T., Bouzguenda, M., Gastli, A. and Masmoudi, A., 2012. MATLAB / Simulink based modelling of solar photovoltaic cell, International Journal of Renewable. Energy Research, 2, 2, 6-9.

63. Zhao, Y., 2010. Fault analysis in solar photovoltaic arrays, Master thesis, Northeastern University Boston, Massachusetts.

64. Hariharan, R., Chakkarapani, M., Saravana Ilango, G., and Nagamani, C., 2016. A method to detect photovoltaic array faults and partial shading in pv systems, IEEE Journal of Photovoltaics, 6, 5, 1278–1285.

65. URL-5 < https://www.ossila.com/pages/organic-photovoltaics-vs-2nd-gen-solar-cell-tech. > Date of access:10.05.2020.

66. Solanki, P.C., 2008. Solar photovoltaic technologies, The Sun and PV technologies. First Edition, Springer.

67. URL-6 < https://www.pilkington.com/en/global/commercial-applications/types-of-glass/solar-energy/solar-technologies/crystalline-silicon-photovoltaics> Date of access:10.12.2019.

68. Fadhel, S., 2019. PV shading fault detection and classification based on I-V curve using principal component analysis: Application to isolated PV system, Solar Energy, 179, 12, 1–10.

69. Jean, J., Brown, P.R., Jaffe, R.L., Buonassisi, T. and Bulović, V., 2015. Pathways for solar photovoltaics, Energy Environ. Sci., 8, 4, 1200–1219.

70. Cosgun A.E. and Uzun, Y., 2017. Thermal fault detection system for pv solar modules, Electrical and Electronic. Engineering: An International Journal, 6, 3, 9–15.

71. Zsiborács, H., 2018. Comparison of thermal models for ground-mounted south-facing photovoltaic technologies: A practical case study, Energies, 11, 5, 1–18.

72. URL-7 < https://link.springer.com/book/10.1007%2F978-981-15-1532-3> Date of access:10.03.2020.

73. URL-8 < http://educypedia.karadimov.info/library/FactSheet-11.pdf> Date of access: 20.12.2019.

74. Oku, T., 2017. 3. Basics of solar cells, Solar Cells and Energy Materials, Gruyter, 40-55.

75. Yerebakan, M., 2010. Güneş enerjisi kullaniminin tarihsel gelişimi ve türkiye'deki yeri, Hyperlink, 1, 1, 36-38.

76. Madeti, S. R. and Singh, S. N., 2017. A comprehensive study on different types of faults and detection techniques for solar photovoltaic system, Solar Energy, 158, 8, 161–185.

77. URL-9 < https://www.electronicshub.org/bypass-diodes-in-solar-panels> Date of access:10.05.2020.

78. Bulanyi, P. and Zhang, R., 2014. Shading analysis and improvement for distributed residential grid- connected photovoltaics systems 2 . shading types, Sol The 52nd Annual Conference Australian Solar Council, 1–12.

79. URL-10 < https://www.petaaerial.com> Date of access:01.12.2019.

80. URL-11 < https://iea-pvps.org/wp-content/uploads/2020/01/IEA-PVPS_T13-01_2014_Review_of_Failures_of_Photovoltaic_Modules_Final.pdf > Date of access: 20.1.2020.

81. Sugimura, R.S., Mon, G.R., Wen, L. and . Ross, R. G., 2003. Electrical isolation design and electrochemical corrosion in thin-film photovoltaic modules, Conference Record of the Twentieth IEEE Photovoltaic Specialists Conference 02, 1103–1109.

82. Kaplani, E., 2012. Detection of degradation effects in field-aged c-si solar cells through ir thermography and digital image processing, International Journal of Photoenergy, 01, 3, 1–11.

83. Sharma, V. and Chandel, S.S., 2013. Performance and degradation analysis for long term reliability of solar photovoltaic systems : A review, Renewable Sustainable Energy Reviews, 27, 6, 753–767.

84. Cristaldi, L., 2015. Diagnostic architecture : A procedure based on the analysis of the failure causes applied to photovoltaic plants, Measurement, 67, 4, 99–107.

85. Kobi, A.C., Ke, M.F., Ndiaye, P.A. and Sambou, V., 2013. Degradations of silicon photovoltaic modules : A literature review, Solar Energy, 96, 11,140–151.

86. Ahmadipour, M., Hizam, H., Othman, M. L., Mohd Radzi, M. A. and Chireh, N. A fast fault identification in a grid-connected photovoltaic system using wavelet multi-resolution singular spectrum entropy and support vector machine, Energies, 12, 13, 10-17.

87. Chaibi, Y., Malvoni, M., Chouder, A., Boussetta, M. and Salhi, M., 2019. Simple and efficient approach to detect and diagnose electrical faults and partial shading in photovoltaic systems, Energy Conversion Management, 196, 2, 330–343.

88. Yilmaz, M., Kayabasi, E. and Akbaba, M., 2019. Determination of the effects of operating conditions on the output power of the inverter and the power quality using an artificial neural network, Engineering. Science and Technololy an International Journal, 2,10, 20-26.

89. Khordehgah, N ., Guichet, V., Lester, S.P. and Jouhara, H., 2019. Computational study and experimental validation of a solar photovoltaics and thermal technology, Renewable Energy, 143, 1, 1348–1356.

90. Dhimish, M., 2018. Fault detection and performance analysis of photovoltaic installations, Ph.D. thesis, The University of Huddersfield, Huddersfield.

91. Orkisz, M. 2018. Estimating Effects of Individual PV Panel Failures on PV Array Output, IEEE Transactions on Industry Applications, 54, 5, 4825–4832.

92. Sebbagh, T., Kelaiaia, R. and Zaatri, A., 2018. An experimental validation of the effect of partial shade on the I-V characteristic of PV panel, International Journal of Advanced Manufacturing Technology, 96, 9, 4165–4172.

93. Madeti, S. R. and Singh, S.N., 2018. Modeling of PV system based on experimental data for fault detection using kNN method, Solar Energy, 01,6,20-27.

94. Belik, M., 2017. Simulation of photovoltaic panels thermal features, 18th International Scientific Conference on Electric Power Engineering EPE 2017, 4, 1–5.

95. Elibol, E., Özmen, Ö. T., Tutkun, N. and Köysal, O., 2017. Outdoor performance analysis of different PV panel types, Renewable. Sustainable. Energy Reviews, 67, 651–661.

96. Mallor, F., León, T., De Boeck, L., Van Gulck, S., Meulders, M. and Van Der Meerssche, B., 2017. A method for detecting malfunctions in PV solar panels based on electricity production monitoring, Solar Energy, 153, 51–63.

97. Wang, Y., Itako, K., Kudoh, T., Koh, K. and Ge, Q., 2017. Voltage-based hot-spot detection method for photovoltaic string using a projector, Energies, 10, 2, 1-7.

98. Harrou, F. , Sun, Y. and Saidi A., 2017. Online Model-based Fault Detection for Grid Connected PV Systems Monitoring, The 5th International Conference on Electrical Engineering-Boumerdes (ICEE-B), 2-8.

99. Kichou S., 2017. Automatic supervision of PV systems and degradation analysis of thin film PV modules, Ph.D. thesis, University Politècnica de Cataluny, Barselona.

100. Dhimish, M., Holmes, V., Mehrdadi, B. and Dales, M., 2017. Diagnostic method for photovoltaic systems based on six layer detection algorithm, Electronics. Power System Research, 151, 26–39.

101. Quaschning, V. and Hanitsch, R., 1995. Numerical simulation of photovoltaic generators with shaded cells, 30th Universities Power Engineering Conference, 0, 583–586.

102. Gow, J. A. and Manning, C. D., 1999. Development of a photovoltaic array model for use in power-electronics simulation studies, IEE Proceedings - Electric Power Applications, 146, 2, 193.

103. Marc, K., Sarah, K. and Corinne, P., 2015. Pvps, Review of Failures of Photovotaic, 1911.

104. Wasif, M., 2015. A Compact , High Precision Position Sensing Embedded System for Fast Steering Mirror, M . Sc . Thesis, Delft University of Technology Department of Computer Engineering, Netherlands.

105. Lee, K., 2016. Building a simple functional near infrared spectroscopy system using Arduino, M . Sc . Thesis, Drexel University, Master of Science in Biomedical Engineering.

106. Liu, F., 2014. Ultra-Violet degradation behavior of polymeric backsheets for photovoltaic modules, Solar Energy, 108 ,10, 88-100.

107. Liu, F., Jiang, L. and Yang, S., 2014. Ultra-violet degradation behavior of polymeric backsheets for photovoltaic modules, Solar Energy, 108, 10, 88–100.

108. Nguyen, D.D. and Lehman, B., 2006. Modeling and simulation of solar PV arrays under changing illumination conditions, Proc. IEEE Workshop on Computers in Power Electronics COMPEL, 295–299.

109. Haque, A.K., Bharath, V.S., Khan, M.A., Khan, I. and Jaffery, Z.A., 2019. Fault diagnosis of Photovoltaic Modules, Energy Science Engineering, 7, 3, 622–644.

110. Ballestín-Fuertes J., 2020 Novel utility-scale photovoltaic plant electroluminescence maintenance technique by means of bidirectional power inverter controller," Applied Science, 13, 10, 1-9.

111. Boppana, S., Rajasekar, V. and Tamizhmani, G., 2015. Working towards the development of a standardized artificial soiling method, 2015 IEEE 42nd Photovoltaic. Specialist Conference PVSC 2015, 1–6.

112. URL-12 <https://www.enerji.gov.tr/tr-TR/Sayfalar/Elektrik> Date of access: 20.01.2020.

113. URL-13 < https://www.iea.org/data-and-statistics/data> Date of access: 02.01.2019.

APPENDIX LIST

APPENDIX A-1:

<table>
<tr><th>Fault Case</th><th>Block</th><th>Power-Voltage Graphs</th><th>Current-Voltage Graphs</th></tr>
<tr><td>a) Normal Module</td><td>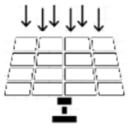</td><td>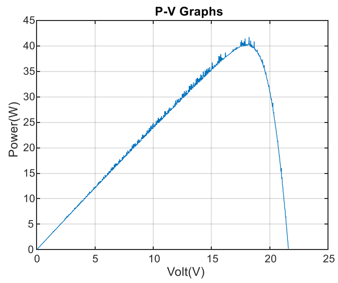
</td><td>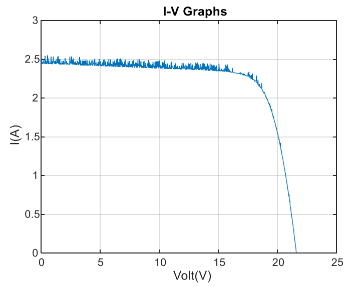
</td></tr>
<tr><td>b) Shading Case</td><td>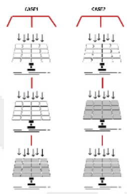</td><td>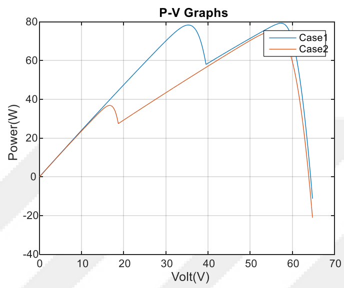
</td><td>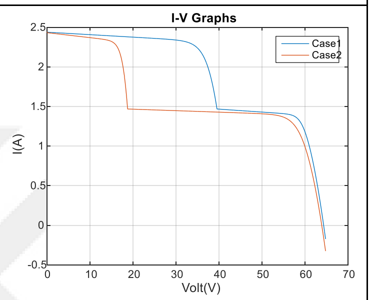
</td></tr>
<tr><td>c) Line to Line</td><td>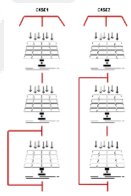</td><td>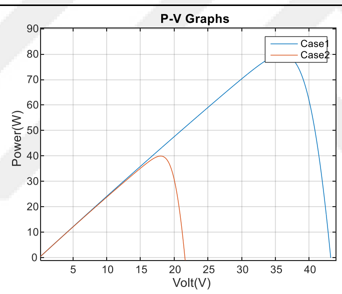
</td><td>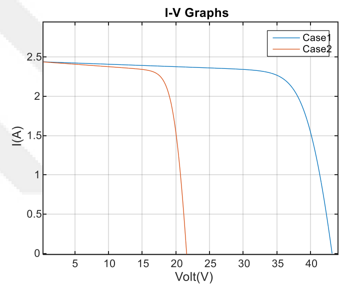
</td></tr>
<tr><td>e) Soiling</td><td>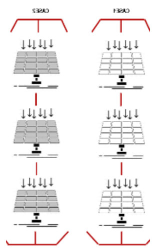</td><td>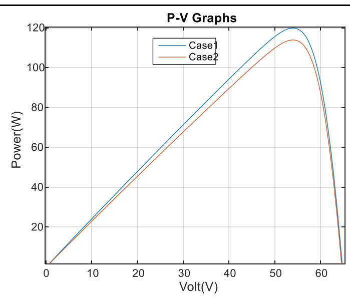
</td><td>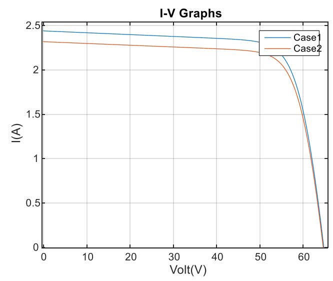
</td></tr>
<tr><td>f) Inc. in Resistance</td><td>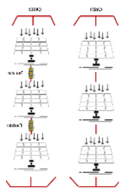</td><td>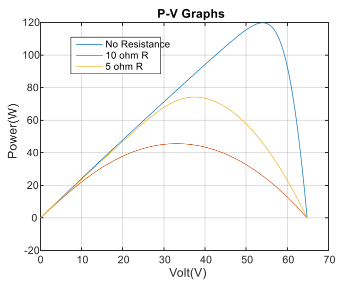
</td><td>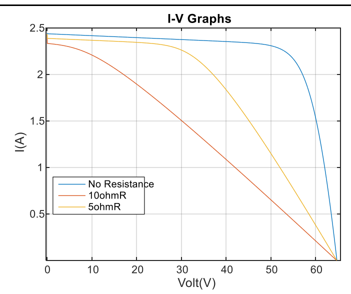
</td></tr>
</table>

g) Bird Droppings Tree Leaves	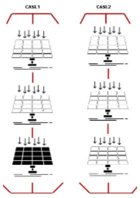	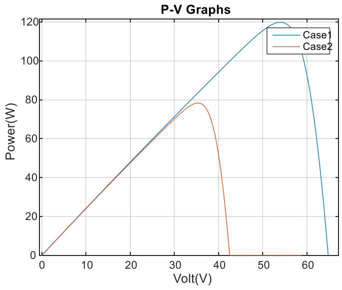	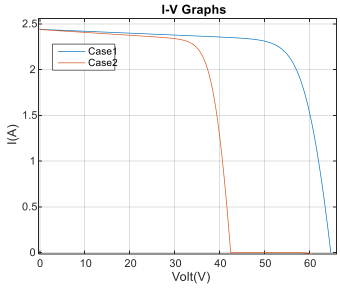
h) Temp. Impact	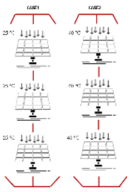	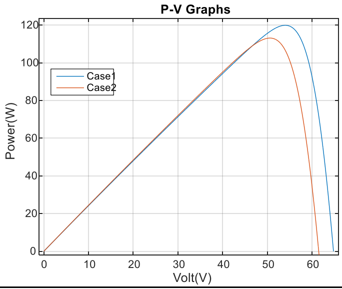	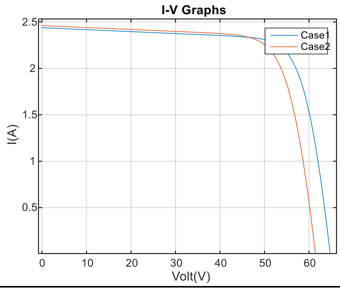

APPENDIX A-2:

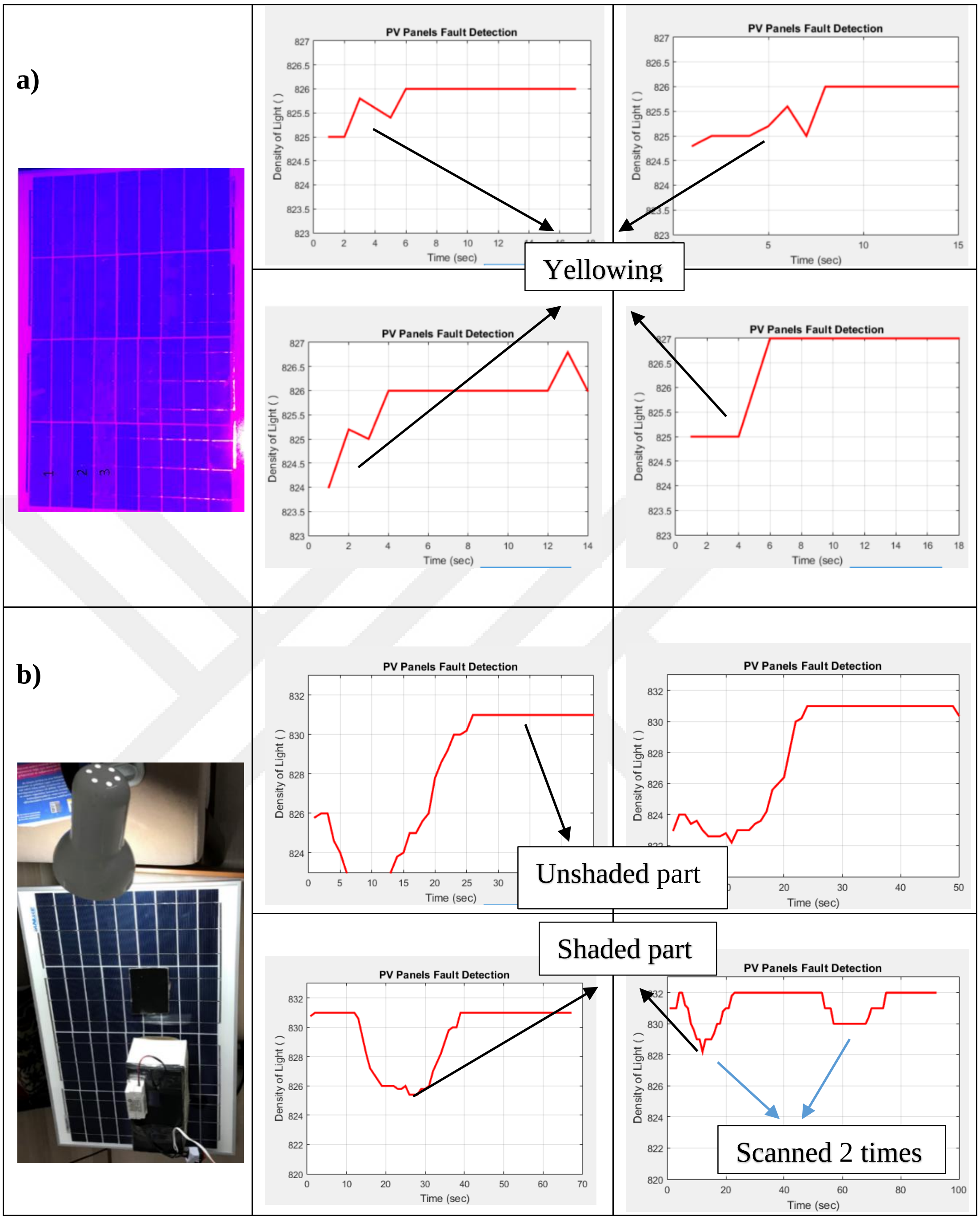

a)
PV Panels Fault Detection
Density of Light ( )
Time (sec)
PV Panels Fault Detection
Density of Light ( )
Time (sec)
Yellowing
PV Panels Fault Detection
Density of Light ( )
Time (sec)
PV Panels Fault Detection
Density of Light ( )
Time (sec)
b)
PV Panels Fault Detection
Density of Light ( )
Time (sec)
PV Panels Fault Detection
Density of Light ( )
Time (sec)
Unshaded part
Shaded part
PV Panels Fault Detection
Density of Light ( )
Time (sec)
PV Panels Fault Detection
Density of Light ( )
Time (sec)
Scanned 2 times

APPENDIX B-1:

Microcontroller	ATmega328
Operating	Voltage 5V
Input Voltage (recommended)	7-12V
Input Voltage (limits)	6-20V
Digital I/O Pins	14 (of which 6 provide PWM output)
Analog Input Pins	6
DC Current per I/O Pin	40 mA
DC Current for 3.3V Pin	50 mA
Flash Memory	32 KB
SRAM	2 KB
EEPROM	1 KB
Clock Speed	16 MHz

APPENDIX B-2:

Viewing Angle	120degree
Forward Voltage	3V
Current	350mA
Thermal Resistance	15℃/W
Wavelength	390nm - 410nm

APPENDIX C-1:

```
int sensorPin = A0;
int okumalar[10];
int toplam=0;

void setup()
{
Serial.begin(9600);
}

void loop()
{
  for(int i=0;i=<9; i++)
  {
  okumalar[i] = analogRead(sensorPin);
  toplam=toplam+okumalar[i];
  }
toplam=toplam/10;
Serial.println( toplam);
delay(140);
}
```

APPENDIX C-2:

```
function varargout = UV_Fault_Detect(varargin)
gui_Singleton = 1;
gui_State = struct('gui_Name',       mfilename, ...
                   'gui_Singleton',  gui_Singleton, ...
                   'gui_OpeningFcn',
@UV_Fault_Detect_OpeningFcn, ...
                   'gui_OutputFcn',
@UV_Fault_Detect_OutputFcn, ...
                   'gui_LayoutFcn',  [] , ...
                   'gui_Callback',   []);
if nargin && ischar(varargin{1})
    gui_State.gui_Callback = str2func(varargin{1});
end

if nargout
    [varargout{1:nargout}]    =    gui_mainfcn(gui_State,
varargin{:});
else
    gui_mainfcn(gui_State, varargin{:});
end

function  UV_Fault_Detect_OpeningFcn(hObject,  eventdata,
handles, varargin)
handles.output = hObject;
guidata(hObject, handles);

function  varargout  =  UV_Fault_Detect_OutputFcn(hObject,
eventdata, handles)
varargout{1} = handles.output;

function     pushbutton1_Callback(hObject,     eventdata,
handles)
if ~isempty(instrfind)
     fclose(instrfind);
      delete(instrfind);
end

comport = serial('COM3');
set(comport, 'BaudRate', 9600);
set(comport, 'DataBits',8);
set(comport, 'Parity', 'none');
set(comport, 'StopBits', 1);
set(comport,'FlowControl','none');
fopen(comport);
pause(2)

x=0;
```

```
set(handles.pushbutton2,'UserData',0);

while (1)

    if get(handles.pushbutton2,'UserData')==1
        break
    else
        dx = fscanf(comport,'%d')
        set(handles.edit1,'string', [num2str(dx)]);
        pause(0.02);

        x=x+1;
        for i=1:1:5
            y(x)=fscanf(comport,'%d');
            y(i)=y(x);
        end

        d(x)= (y(1)+y(2)+y(3)+y(4)+y(5))/5;
        drawnow;
        axes(handles.axes1);
        plot(d,'r','linewidth',2
        grid on
        title('PV Panels Fault Detection');
        xlabel('Time (sec)');
        ylabel('Density of Light ( )');
        ylim([820 833]) %
    end
end
fclose(comport);
delete(comport)
clear comport

function     pushbutton2_Callback(hObject,     eventdata,
handles)
set(handles.pushbutton2,'UserData',1);

function edit1_Callback(hObject, eventdata, handles)

function edit1_CreateFcn(hObject, eventdata, handles)
if   ispc   &&   isequal(get(hObject,'BackgroundColor'),
get(0,'defaultUicontrolBackgroundColor'))
    set(hObject,'BackgroundColor','white');
end

function axes2_CreateFcn(hObject, eventdata, handles)
degisken = image(imread ( 'panel.jpg ' ) )
set(gca,'visible','off');
```

CURRICULUM VITAE

Name and Surname : Atıl Emre COŞGUN

Address : Nakkaş Mah., 2830. Sok., Vizyon1 Merkez/AKSARAY

E-mail address : atilcosgun@gmail.com

EDUCATION INFORMATION

Undergraduate : Atılım University, 2005-2010

Master : Karabük University, 2011-2014

Ph.D. : Aksaray University, 2016-2020

PROFESSIONAL EXPERIENCE AND AWARDS

1. Uzmar Shipbuilding and Trade Inc. (2008) / Intern
2. Ford Otosan (2009) / Intern
3. AGE Otomation / R&D Engineer (2010-2011)
4. Karabük University /Research Assistant (2011-2016)
5. Artes Robotic (2015-) / Supported in TÜBİTAK 1512 Techno-Enterprise Capital Support
6. Aksaray University (2016-)
7. Best vehicle design award in TUBITAK Electromobile Category-2014
8. METU in Robot Competitions 1. Awarded –Free style category (2-TEA)-2009

PUBLICATIONS, PRESENTATIONS AND PATENTS

1. Coşgun, A. E. and Uzun, Y, 2017. Thermal fault detection system for Pv solar modules, International Journal of Electronics and Electrical Engineering, 6, 3, 09–15.

2. Coşgun, A. E. and Tolun, M. R, 2019. Academic studies in engineering, architecture, planning and design sciences-2019/2, Journal of Chemical Information and Modeling, 1, 2, 212–229.